COPERNICUS
MARINE ENVIRONMENT MONITORING SERVICE

QUALITY INFORMATION DOCUMENT

Mediterranean Production Centre
MEDSEA_ANALYSIS_FORECAST_WAV_006_017

Issue: 1.3

Contributors: Anna Zacharioudaki, Michalis Ravdas, Gerasimos Korres

Approval date by the CMEMS product quality coordination team:

CHANGE RECORD

When the quality of the products changes, the QuID is updated and a row is added to this table. The third column specifies which sections or sub-sections have been updated. The fourth column should mention the version of the product to which the change applies.

Issue	Date	§	Description of Change	Author	Validated By
1.2	January 2019	All	Release of the new version (MEDWAM3) of the Med-waves analysis and forecast product at 1/24º resolution. Upgrades since previous version (Q2/2018) include: i) upgrade of WAM model version from V4.5.4 to V4.6.2, ii) inclusion of non-linear wave-wave interactions for shallow water, iii) tuning of WAM input and dissipation source terms, and iv) tuning of spectral steepness.	Anna Zacharioudaki	Vladyslav Lyubartsev (PQ Responsible)
1.3	December 2019	I.3, II.1, II.2, V, VI	Updates of the new version Q1/2020 with respect to the previous version Q1/2019 include: i) daily forecast cycle starting at 00:00 UTC instead of 12:00 UTC. This is a technical change with no changes in product quality, and ii) additional assimilation of SENTINEL-3B observations. Quality changes are marginal and are described in Section VI.	Anna Zacharioudaki	

Table of contents

I EXECUTIVE SUMMARY

I.1 Products covered by this document

This document describes the quality of the analysis and forecast nominal product of the wave component of the Mediterranean Sea: MEDSEA_ANALYSIS_FORECAST_WAV_006_017. The product includes the following 2D 1-hourly analysis and forecast instantaneous fields of:

- VHMO: spectral significant wave height (Hm0);
- VTM10: spectral moments (-1,0) wave period (Tm-10);
- VTM02: spectral moments (0,2) wave period (Tm02);
- VTPK: wave period at spectral peak / peak period (Tp);
- VMDR: mean wave direction from (Mdir);
- VPED: wave principal direction at spectral peak;
- VSDX: stokes drift U;
- VSDY: stokes drift V;
- VHM0_WW: spectral significant wind wave height;
- VTM01_WW: spectral moments (0,1) wind wave period;
- VMDR_SW1: mean wind wave direction from;
- VHM0_SW1: spectral significant primary swell wave height;
- VTM01_SW1: spectral moments (0,1) primary swell wave period;
- VMDR_SW1: mean primary swell wave direction from;
- VHM0_SW2: spectral significant secondary swell wave height;
- VTM01_SW2: spectral moments (0,1) secondary swell wave period; and
- VMDR_SW2: mean secondary swell wave direction from.

Output data are produced at 1/24° horizontal resolution.

I.2 Summary of the results

The quality of the MED-MFC-waves system of analysis and forecast is assessed over a 1 year period (2016) by comparison with in-situ and satellite observations.

The main results of the MEDSEA_ANALYSIS_FORECAST_WAV_006_017 product quality assessment are summarized below:

Spectral Significant Wave Height (Hm0): Overall, the significant wave height is accurately simulated by the model. Considering the Mediterranean Sea as a whole, the typical difference with observations (RMSD) is 0.2-0.21 m with a bias ranging from 0 m to -0.03 m (3%) depending on the source of observations the model is compared against. In general, the model somewhat underestimates or converges to the observations for wave heights smaller than about 2 m whilst it mostly overestimates or converges to the observations for higher waves. Its performance is better in winter when the wave conditions are well-defined. Spatially, the model performs optimally at offshore wave buoy locations and well-exposed Mediterranean sub-regions. Within enclosed basins and near the coast, unresolved

topography by the wind and wave models and fetch limitations cause the wave model performance to deteriorate.

Spectral moments (0,2) wave period (Tm02): The mean wave period is reasonably well simulated by the model. The typical difference with observations (RMSD) is 0.69 s and is mainly caused by model bias which has a value of -0.49 s (12%). In general, the model underestimates the observed mean wave period and exhibits greater variability than the observations. A relatively larger model underestimate is found for mean wave periods below 4.5 s. Over the high MWP range the model tends to converge or even overestimate the observed values. Model performance is a little better in winter when wave conditions are well-defined. Similarly to the wave height, the model performance is best at well-exposed offshore locations and deteriorates near the shore mainly due to fetch limitations.

Other variables: No observations are available for all other variables except for the wave period at spectral peak / peak period (Tp) and the mean wave direction from (Mdir). In contrast to Tm02 variation, which is smooth in the Mediterranean Sea, Tp variation is particularly spiky. As a result, validation of the latter wave parameter is thought to be less reliable and has not been considered herein despite data availability. On the other hand, qualification of Mdir will be considered in the future. Generally, wave height variables are expected to be of similar quality to Hm0 and wave period variables to Tm02. Stokes drift quality is expected to be a function of both Hm0 and Tm02.

I.3 Estimated Accuracy Numbers

Estimated Accuracy Numbers (EANs), that are the mean and the RMS of the differences (RMSD) between the model and in-situ or satellite reference observations, are provided in Table 1 and Table 2 below.

EANs are computed for:

- Significant Wave Height (SWH): refers to the "spectral significant wave height (Hm0)"
- Mean Wave Period (MWP): refers to the "spectral moments (0,2) wave period (Tm02)"

The observations used are:

- independent in-situ observations from moored wave buoys obtained from the CMEMS INSITU_MED_NRT_OBSERVATIONS_013_035 dataset, available through the CMEMS In Situ Thematic Assemble Centre (INS-TAC)
- quasi-independent satellite altimeter observations from a merged altimeter wave height database setup at CERSAT - IFREMER

	Q2/2018		Q1/2019			
Model vs. in-situ observations: full MED	**BIAS**	**RMSD**	**BIAS**	**RMSD**	Units	Decimal places
SWH	-0.005	0.2	-0.004	0.202	m	3
MWP	-0.55	0.727	-0.488	0.693	s	3

Table 1: EANs of SWH and MWP evaluated for a period of 1 year (2016) for the full Mediterranean Sea: SWH-H-CLASS2-MOOR-BIAS-MED, SWH-H-CLASS2-MOOR-RMSD-MED, MWP-H-CLASS2-MOOR-BIAS-MED, MWP-H-CLASS2-MOOR-RMSD-MED in Table 4, Section III.

	Q2/2018		Q1/2019			
Model SWH vs. satellite observations: full MED and sub-regions	**BIAS**	**RMSD**	**BIAS**	**RMSD**	Units	Decimal places
MED	-0.037	0.214	-0.031	0.214	m	3
atl	0.058	0.209	0.043	0.209		
alb	0.035	0.217	0.039	0.221		
swm1	-0.006	0.232	-0.004	0.232		
swm2	-0.023	0.242	-0.020	0.242		
nwm	-0.034	0.229	-0.030	0.230		
tyr1	-0.032	0.213	-0.029	0.214		
tyr2	-0.029	0.213	-0.024	0.214		
ion1	-0.033	0.207	-0.027	0.208		
ion2	-0.042	0.220	-0.035	0.219		
ion3	-0.059	0.208	-0.055	0.208		
adr1	-0.083	0.242	-0.077	0.241		
adr2	-0.077	0.220	-0.072	0.219		
lev1	-0.043	0.199	-0.034	0.198		
lev2	-0.048	0.189	-0.042	0.187		
lev3	-0.044	0.183	-0.036	0.179		
lev4	-0.057	0.199	-0.053	0.198		
aeg	-0.020	0.212	-0.012	0.214		

Table 2: EANs of SWH evaluated for a period of 1 year (2016) for the full Mediterranean Sea and the different sub-regions shown in Figure 1: SWH-H-CLASS4-ALT-BIAS-MED, SWH-H-CLASS4-ALT-BIAS-MED, SWH-H-CLASS4-ALT-BIAS-<REGIONS>, SWH-H-CLASS4-ALT-RMSD-<REGIONS> in Table 4, Section III.

The EANs are provided for the Q2/2018 and Q1/2019 versions of the CMEMS Mediterranean Sea wave modelling system. The following and newest version of the Med-waves system (Q1/2020) includes a technical change which does not affect the quality of the product and a change in the assimilated datasets which introduced only marginal quality changes outlined in Section VI of this document. The computed EANs are based on the simulation of the system in analysis or first-guess mode depending on the reference data used, for a period of 1 year from 01 January 2016 to 31 December 2016. They are computed for the Mediterranean Sea as a whole and for 17 sub-regions from which 1 is in the Atlantic Ocean and 16 in the Mediterranean Sea (Figure 1): (atl) Atlantic, (alb) Alboran Sea, (swm1) West South-West Med, (swm2) East South-West Med, (nwm) North West Med, (tyr1) North Tyrrhenian Sea, (tyr2) South Tyrrhenian Sea, (adr1) North Adriatic Sea, (adr2) South Adriatic Sea, (ion1)

South-West Ionian Sea, (ion2) South-East Ionian Sea, (ion3) North Ionian 3, (aeg) Aegean Sea, (lev1) West Levantine, (lev2) North-Central Levantine, (lev3) South-Central Levantine, (lev4) East Levantine.

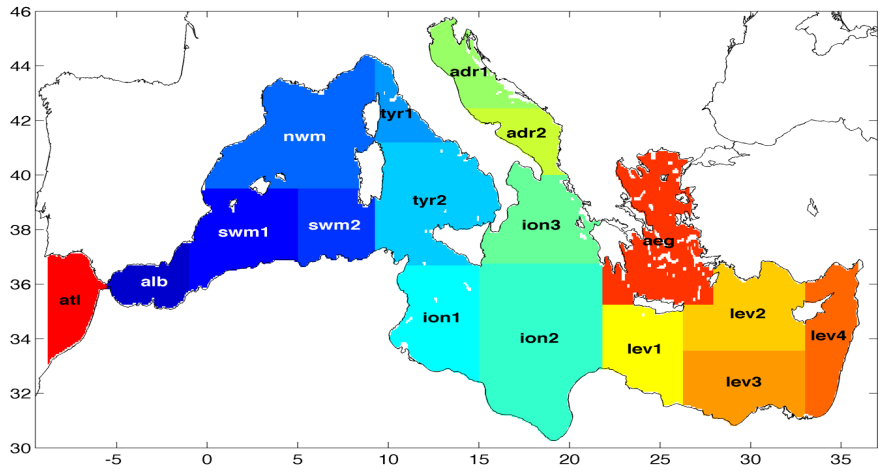

Figure 1: Mediterranean Sea sub-regions for qualification metrics

II PRODUCTION SYSTEM DESCRIPTION

II.1 Production centre details

PU: HCMR, Greece

Production chain: Med-waves

External product (2D): spectral significant wave height (Hm0), spectral moments (-1,0) wave period (Tm-10), spectral moments (0,2) wave period (Tm02), wave period at spectral peak / peak period (Tp), mean wave direction from (Mdir), wave principal direction at spectral peak, stokes drift U, stokes drift V, spectral significant wind wave height, spectral moments (0,1) wind wave period, mean wind wave direction from, spectral significant primary swell wave height, spectral moments (0,1) primary swell wave period, mean primary swell wave direction from, spectral significant secondary swell wave height, spectral moments (0,1) secondary swell wave period, mean secondary swell wave direction from.

Frequency of model output: 1-hourly analysis and forecast (instantaneous)

Geographical coverage: 18.125°W → 36.2917°E; 30.1875°N → 45.9792°N

Horizontal resolution: 1/24°

Vertical coverage: Surface

Length of forecast: 10 days

Frequency of forecast release: Daily

Analyses: Yes

Frequency of analysis release: Daily

The wave analyses and forecasts for the Mediterranean Sea are produced by the HCMR Production Unit by means of the WAM wave model (described below).

The Med-waves system is run once per day starting at 00:00:00 UTC. It produces 10-day (240 h) forecast fields initialized by 1-day (24 h) of analysis where satellite along-track SWH observations are assimilated into the model. A schematic of the Med-waves operational cycle is shown in Figure 2.

The Med-waves system integration is composed of several steps:

1. Upstream Data Acquisition, Pre-Processing and Control of: ECMWF (European Centre for Medium-Range Weather Forecasts) NWP (Numerical Weather Prediction) atmospheric forcing, CMEMS Med MFC and Global MFC currents and CMEMS WAVE TAC SWH satellite NRT observations.
2. Analysis/Forecast: WAM produces one day of analysis forced with ECMWF 6-hourly analyses winds and assimilating along track SWH observations and 10 days of forecast.
3. Post processing: the model output is processed in order to obtain the products for the CMEMS catalogue.
4. Output delivery.

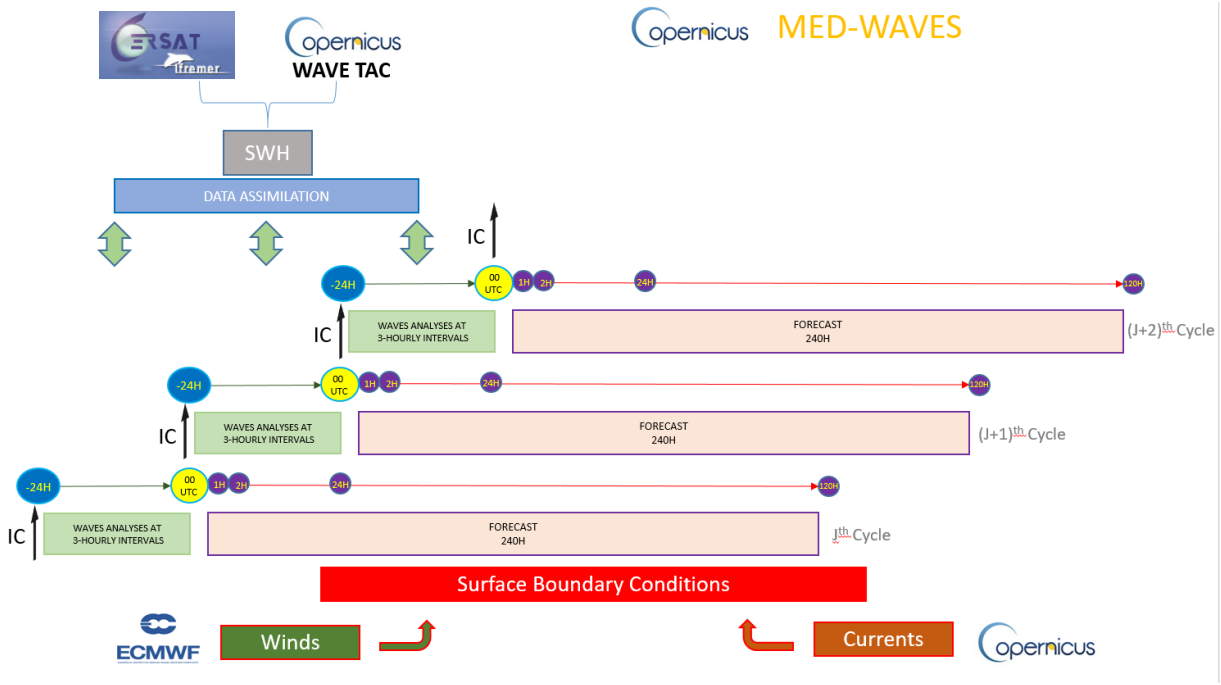

Figure 2: Schematic of the Med-waves operational cycle: 240-h forecasts are initialized daily with initial conditions (IC) taken from the analysis run of the previous day.

II.2 Description of the Med-waves modelling system

The wave component of the Mediterranean Forecasting Centre (Med-waves) is providing analyses and short-term wave forecasts (10 days) for the Mediterranean Sea at 1/24° horizontal resolution.

The Med-waves modelling system consists of a wave model grid implemented over the whole Mediterranean Sea at 1/24° horizontal resolution nested within a coarser resolution wave model grid implemented over the Atlantic Ocean (Figure 3).

Med-waves is based on the state-of-the-art third-generation wave model WAM Cycle 4.6.2 which is a modernized and improved version of the well-known and extensively used WAM Cycle 4 wave model (WAMDI Group, 1988; Komen et al., 1994). Compared to the previous version of the WAM model (Cycle 4.5.4) used in the Q1/2018 version of the Med-waves system, WAM Cycle 4.6.2 includes the following improvements: 1) different depth scaling (deep – shallow) for the calculation of the nonlinear wave-wave interactions is possible and 2) some updates in the subroutines which calculate the wave parameters (i.e Stokes Drift, Hmax).

WAM solves the wave transport equation explicitly without any presumption on the shape of the wave spectrum. Its source terms include the wind input, whitecapping dissipation, nonlinear transfer and bottom friction. The wind input term is adopted from Snyder et al. (1981). The whitecapping dissipation term is based on Hasselmann (1974) whitecapping theory. The wind input and whitecapping dissipation source terms of the present cycle of the wave model are a further development based on Janssen´s quasi-linear theory of wind-wave generation (Janssen, 1989; Janssen, 1991). The nonlinear transfer term is a parameterization of the exact nonlinear interactions as proposed by Hasselmann and Hasselmann (1985) and Hasselmann et al., (1985). Lastly, the bottom friction term is based on the empirical JONSWAP model of Hasselmann et al. (1973).

The Med-waves set-up includes a coarse grid domain with a resolution of 1/6° covering the North Atlantic Ocean from 75°W to 10°E and from 10°N to 70°N and a nested fine grid domain with a resolution of 1/24° covering the Mediterranean Sea from 18.125°W to 36.2917°E and from 30.1875°N to 45.9792°N. The areas covered by the two grids are shown in Figure 3.

The bathymetric map has been constructed using the GEBCO bathymetric data set for the Mediterranean Sea model and the ETOPO 2 data set (U.S. Department of Commerce, National Oceanic and Atmospheric Administration, National Geophysical Data Centre, 2006. 2-minute Gridded Global Relief Data) for the North Atlantic model. In both cases mapping on the model grid was done using bi-linear interpolation accompanied by some degree of isotropic laplacian smoothing.

The Mediterranean Sea model receives full wave spectrum at 3-hourly intervals at its Atlantic Ocean open boundary from the North Atlantic model. The latter model is considered to have all of its four boundaries closed assuming no wave energy propagation from the adjacent seas. This assumption is readily justified for the north and west boundaries of the North Atlantic model considering the adjacent topography which restricts the development and propagation of swell into the model domain. The choice of the south boundary location is less obvious and is based on a number of studies which agree that no important swell energy is expected to propagate northwards from geographical areas south of 10°N. Specifically, according to Semedo et al. (2011), a swell front present in all seasons can be identified in the Atlantic Ocean within the latitude band from 15°S (Dec-Jan-Feb) to 15°N (Jun-Jul-Aug). Young (1999) suggests this swell front never migrates north of the equator. The relatively narrow geometry of the Atlantic restricts propagation of Southern Ocean swell into the Northern Hemisphere. According to Alves (2006) storms within the extratropical South Atlantic ocean (below 40

°S) typically propagate to the east spreading swell energy to the Indian Ocean. As for the Atlantic tropical areas, storms rarely evolve in the south band (between 20°S and the equator) while in the north tropical band (between the equator and 20°N) summer storms move mostly westwards. During winter, the north tropical band can be affected by eastward propagating North Atlantic extratropical storms generating swells that propagate to the southeast (Alves, 2006).

The wave spectrum is discretized using 32 frequencies, which cover a logarithmically scaled frequency band from 0.04177 Hz to 0.8018 Hz (covering wave periods ranging from approximately 1 s to 24 s) at intervals of df/f = 0.1, and 24 equally spaced directions (15 degrees bin).

The Mediterranean model runs in shallow water mode considering wave refraction due to depth and currents in addition to depth induced wave breaking. The North Atlantic model runs in deep water mode with wave refraction due to currents only. The North Atlantic model additionally considers wave energy damping due to the presence of sea ice. A model grid point is considered to be a sea ice point if the ice fraction at that point exceeds 60%. At all sea ice points the wave energy is set to zero.

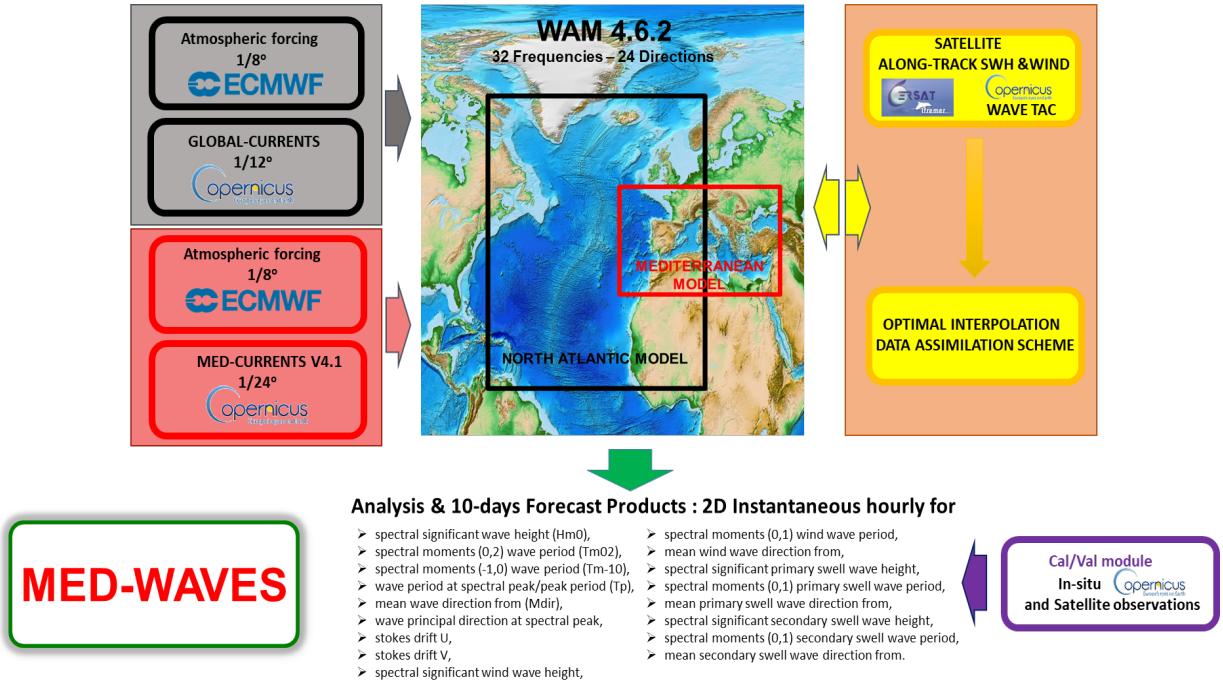

Figure 3: Schematic of the Med-waves system (MEDWAM3).

Modifications from default values have been performed in the input source functions. Specifically, the value of the wave age parameter (zalp) has been set to 0.011 (0.008 is the default) for the Mediterranean model. In addition, the imposition of a limitation to the high frequency part of the wave spectrum corresponding to the latest version of the ECMWF wave forecasting system (ECMWF, 2016) has been applied in order to reduce the wave steepness at very high wind speeds.

The system is forced with 10 m above sea surface wind fields obtained from the ECMWF Integrated Forecasting System (IFS) at 1/8° dissemination resolution. The temporal resolution of the wind forcing is 3 h for the first 3 days of the forecast and 6 h for the rest of the forecast cycle. The wind is bi-linearly interpolated onto the model grids. Sea ice coverage fields are also obtained from ECMWF at the same horizontal resolution (1/8°) and are updated at daily frequency. With respect to currents forcing, the

Mediterranean Sea model is forced by daily averaged surface currents obtained from CMEMS Med MFC at 1/24° resolution (Q1/2019) and the North Atlantic model is forced by daily averaged surface currents obtained from the CMEMS Global MFC at 1/12° resolution (Q2/2018). These are the CMEMS Global and Med MFC surface currents products operational at the time of release of the Med-waves system. A schematic of the Med-waves system is shown in Figure 3. Also, Table 3 summarizes the Med-waves modelling characteristics. Future upgrades of the Med-waves system will consider coupling to the latest surface currents operational products of CMEMS Global and Med MFC systems.

Med-waves generates hourly wave fields over the Mediterranean Sea at 1/24° horizontal resolution. These wave fields correspond either to wave parameters computed by integration of the total wave spectrum or to wave parameters computed using wave spectrum partitioning. In the latter case the complex wave spectrum is partitioned into wind sea, primary and secondary swell. Wind sea is defined as those wave components that are subject to wind forcing while the remaining part of the spectrum is termed swell. Wave components are considered to be subject to wind forcing when

$$c \leq 1.2 \times 28\, u_* \cos(\theta - \varphi)$$

where c is the phase speed of the wave component, u_* is the friction velocity, θ is the direction of wave propagation and ϕ is the wind direction. As the swell part of the wave spectrum can be made up of different swell systems with quite distinct characteristics it is further partitioned into the two most energetic wave systems, the so called primary and secondary swell. Swell partitioning is done following the method proposed by Gerling (1992) which finds the lowest energy threshold value at which upper parts of the spectrum get disconnected with the process repeated until primary and secondary swell is detected.

The assimilation module

The assimilation system of Med-waves is based on the inherent data assimilation scheme of WAM Cycle 4.6.2 which consists of performing an optimal interpolation (O.I.) on the along-track SWH observations retrieved by the altimeters and then re-adjusting the wave spectrum at each grid point accordingly. This assimilation approach was initially developed by Lionello et al. (1992) and consists of two steps.

First, a best guess (analysed) field of significant wave height is determined by optimum interpolation with appropriate assumptions regarding the error covariance matrix. Based on the prejudice that the wind is the main contributor to the wave model error and that the form of the spectra is essentially correct, the aim is to obtain the spectrum that the model would have if the correct forcing was used. One of the key issues of the optimal interpolation approach is the specification of the errors of the assimilating system. Especially, the specification of the background error covariance matrix, P, and the observation error covariance matrix, R, are important since the computation of the gain matrix K depends largely on the structure of these matrices. The Med-waves assimilation module, uses the default expressions of WAM for the background error covariance matrix

$$P = exp\left(\frac{d_{ij}}{l_c}\right)$$

and the observation error covariance matrix

$$R = \frac{\sigma_o^2}{\sigma_b^2}$$

where *i* and *j* are, respectively, the model grid points, d is the distance from the observation location to the grid point, l_c is the correlation length, while σ_o and σ_b stand for the observation and model errors, respectively. In the above expressions the error is considered as homogeneous and isotropic.

We set the ratio between errors of observations and model (background) equal to 1 and the correlation length l_c which controls the width of exponential bell equal to 3 deg (~300 km).

Finally, the weights assigned to the observations are the elements of the gain matrix *K*:

$$K = PH^T[HPH^T + R]^{-1}$$

where H is the observation operator that projects the model solution to the observation location.

The above O.I. analysis procedure applies to significant wave height and 10 m wind speed, U10, observations that fall within the model domain. For the current version of Med-waves, it has been applied to altimeter along-track SWH measurements only. No assimilation of U10 measurements is performed because of a lack of readily available data. It has been shown, through sensitivity testing, that omitting U10 assimilation in the Mediterranean Sea has negligible effect on output quality.

During the second step, the analysed significant wave height field is used to retrieve the full dimensional wave spectrum from a first-guess spectrum provided by the model itself, introducing additional assumptions to transform the information of a single wave height spectrum into separate corrections for the wind sea and swell components of the spectrum. Two-dimensional wave spectra are regarded either as wind sea spectra, if the wind sea energy is larger than 3/4 times the total energy, or, if this condition is not satisfied, as swell. If the first-guess spectrum is mainly wind-sea, the spectrum is updated using empirical energy growth curves from the model. Additionally, if 10 m winds observations are available the local forcing wind speed is updated. In case of swell, the spectrum is updated assuming the average wave steepness provided by the first-guess spectrum is correct but the wind is not updated. A problem arises when both wind-sea and swell are present. In this situation the update is done depending on which is the dominant process, which is a limitation of the method

Prior to assimilation all altimeter SWH observations are subject to quality control procedure. The primary purpose of the quality control system is to identify observations that are obviously erroneous, as well as the more difficult process of identifying measurements that fall within valid and reasonable ranges but nevertheless are erroneous. Accepting this erroneous data can cause an incorrect analysis, while rejecting extreme, but valid, data can miss important events. The procedure takes into account thresholds of significant wave height and wind speed (upon availability) observations and root mean square differences between the model first-guess and the observed SWH.

Every day the system is restarted at 00:00 UTC of day D-1 and integrated to 23:00 UTC of day D by incorporating all satellite SWH observations available from CMEMS WAVE TAC. The assimilation step adopted for the current version of the Med-waves system equals to 3 hours.

	North Atlantic (Coarse)	Mediterranean Sea (Fine)
Model	WAM Cycle 4.6.2	
Model Domain	-75°E 10°W 10°S 70°N	-18.125°E 36.291°W 30.1875°N 45.9792°N
Horizontal Resolution	1/6° x 1/6°	1/24° x 1/24°
Frequency Bins	32 (logarithmically spaced) 0.04177-0.80818 Hz	
Direction Bins	24 (equally spaced)	
Propagation Time-Step	300 s	60 s
Forcing (10m winds)	1/8° x 1/8° ECMWF operational analysis & 10-days forecasts	
Data assimilation	SWH along-track NRT observations (JASON-3, SENTINEL-3A, SENINTEL-3B, CRYOSAT2, SARAL) from CMEMS WAVE TAC	
Surface Currents	CMEMS GLOBAL MFC (1/12° x 1/12°)	CMEMS MED MFC (1/24° x 1/24°)
Sea Ice	1/8° x 1/8° ECMWF	-

Table 3: Med-waves modelling characteristics

II.3 Upstream data and boundary condition of the WAM model

The CMEMS Med-waves system uses the following upstream data:

1. Atmospheric forcing: NWP 6-h (3-h for the first 3 days of forecast) operational analysis and forecast fields from ECMWF disseminated at 1/8º horizontal resolution, distributed by the Italian National Meteo Service (USAM/CNMA).
2. Data assimilation: WAVE_GLO_WAV_L3_SWH_NRT_OBSERVATIONS_014_001 inter calibrated along track SWH observations from JASON-3, SENTINEL-3A, SENTINEL-3B, SARAL/Altika and CRYOSAT-2 satellite missions, distributed by the CMEMS WAVE TAC.
3. Surface currents forcing: GLOBAL_ANALYSIS_FORECAST_PHY_001_024 daily averages at 1/12º (Atlantic model grid forcing) and MEDSEA_ANALYSIS_FORECAST_PHY_006_013 daily averages at 1/24º (Mediterranean model grid forcing) from the CMEMS Global MFC and the CMEMS Mediterranean MFC Analysis and Forecast Systems respectively.
4. Sea-ice cover: daily analysis fields from ECMWF at 1/8º (remain constant during the operational cycle) distributed by the Italian National Meteo Service (USAM/CNMA).

III VALIDATION FRAMEWORK

In order to evaluate and assure the quality of the MEDSEA_ANALYSIS_FORECAST_WAV_006_017 product of the CMEMS Med-waves, the Med-waves system described in Section II has been integrated in analysis and first-guess mode for year 2016. Model analysis and first-guess outputs were then compared to independent and quasi-independent observations respectively, focusing on output quality in the Mediterranean Sea. It is noted that all the observations that are assimilated into the system are considered as quasi-independent. In this situation, to assure some level of independency, qualification metrics are calculated before the assimilation of data (i.e. first-guess output). It is also highlighted that the qualification run differs from the operational with respect to the data assimilated in the system. This is because the CMEMS satellite observations assimilated in the operational system have not being available over a period of a full year before year 2018. Instead, quality-controlled inter-calibrated data from JASON-2 and SARAL, obtained from CERCAT-IFREMER, have been assimilated. It is noted at this point that JASON-2 has been used to inter-calibrate satellite data from different missions in CERCAT-IFREMER while JASON-3 has been used for the same purpose in CMEMS. According to results from Queffeulou (2016) these two satellites have a very similar performance.

The wave parameters that have been qualified through their comparison with observations include:

- ✓ spectral significant wave height (Hm0) [SWH]
- ✓ spectral moments (0,2) wave period (Tm02) [MWP]

The remaining wave parameters included in the CMEMS Med-waves product are not qualified against observational data. This is mainly because there are no relevant observations or because the existing observations are not suited for a robust validation either because of limited data availability or because of data ambiguities (e.g. highly spiky variation). In most of the cases, the quality of these wave parameters is inferred from the quality of those parameters that are thoroughly compared with observations. A valid range, based on climatology and/or expert knowledge, is assigned to each wave parameter.

The observations against which modelled wave parameters are compared to include:

- independent in-situ observations from moored wave buoys obtained from the CMEMS INSITU_MED_NRT_OBSERVATIONS_013_035 dataset, available through the CMEMS In Situ Thematic Assemble Centre (INS-TAC)
- quasi-independent satellite altimeter observations from a merged altimeter wave height database setup at CERSAT - IFREMER

Significant wave height measurements from 25 wave buoys within the Mediterranean Sea were available in the examined year. Figure 4 depicts their location and unique ID code. Mean wave period measurements were available from 22 of the depicted buoys (see Figure 11). In order to collocate model output and buoy measurements in space, model output was taken at the grid point nearest to the buoy location. In time, buoy measurements within a time window of ± 1 h from model output times at 3-h intervals (0, 3, 6, ..., etc) were averaged. Prior to model-buoy collocation, the in-situ observations were filtered so as to remove those values accompanied by a bad quality flag (Quality Flags included in the data files provided by the INS-TAC). After collocation, visual inspection of the data was carried out, which led to some further filtering of spurious data points. In addition, MWP data

below 2 s were omitted from the statistical analysis, since 0.5 Hz (T = 2 s) is a typical cut-off frequency for wave buoys.

Figure 4: Wave buoys' location and unique ID code

Satellite observations of significant wave height, SWH, and wind speed, U10 (used to validate the forcing wind fields), for year 2016 were obtained from a merged altimeter wave height database setup at CERSAT - IFREMER, France. This database contains altimeter measurements that have been filtered and corrected (Queffeulou and Croizé-Fillon, 2013). Here, measurements from 2 satellite missions, the JASON-2 and SARAL, were used. Available data from CRYOSAT-2 have not been used because of quality discrepancies found for the Mediterranean Sea in relation to the other two missions (Ravdas et al., 2018). To collocate model output and satellite observations the former were interpolated in time and space to the individual satellite tracks. For each track, corresponding to one satellite pass, along-track pairs of satellite measurements and interpolated model output were averaged over ~30 km grid cells, centered at grid points of the wave model. This averaging is intended to break any spatial correlation present in successive 1 Hz (~7 km) observations and/or in neighboring model grid output (Queffeulou, personal communication).

Metrics that are commonly applied to assess numerical model skill and are in alignment with the recommendations of the EU FP7 project MyWave (A pan-European concerted and integrated approach to operational wave modelling and forecasting – a complement to GMES MyOcean services, 2012-2014) have been used to qualify the Med-waves system within the Mediterranean Sea. These include the RMSD, BIAS, Scatter Index (SI), Pearson Correlation Coefficient (CORR), and the Linear Regression Slope and Intercept (LR_SLOPE, LR_INTR). The SI, defined here as the standard deviation of model-observation differences relative to the observed mean, being dimensionless, is more appropriate to evaluate the relative closeness of the model output to the observations at different locations compared with the RMSD which is representative of the size of a 'typical' model-observation difference. In addition to the aforementioned core metrics, merged Density Scatter and Quantile-Quantile (QQ) plots are provided. The full set of metrics used in the qualification of the Med-waves system is defined in Table 4.

Name	Description	Wave parameter	Supporting reference dataset	Quantity
Evaluation of Med-waves using independent in-situ observations (Full MED)				
SWH-H-CLASS2-MOOR-<STAT>-MED	Comparison to wave buoy significant wave height	Spectral significant wave height (Hm0)	INSITU_MED_NRT_OBSERVATIONS_013_035	RMSD, SI, BIAS, CORR, LR_SLOPE, LR_INTR between observations and analysis, for all Med, for 1-year period and seasonally
MWP-H-CLASS2-MOOR-<STAT>-MED	Comparison to wave buoy mean wave period	Spectral moments (0,2) wave period (Tm02)	INSITU_MED_NRT_OBSERVATIONS_013_035	RMSD, SI, BIAS, CORR, LR_SLOPE, LR_INTR between observations and analysis, for all Med, for 1-year period and seasonally
SWH-H-CLASS2-MOOR-QQ-MED SWH-H-CLASS2-MOOR-SCATTER-MED	Comparison to wave buoy significant wave height	Spectral significant wave height (Hm0)	INSITU_MED_NRT_OBSERVATIONS_013_035	Merged Quantile-Quantile and Scatter plots between observations and analysis, for all Med, for 1-year period
MWP-H-CLASS2-MOOR-QQ-MED MWP-H-CLASS2-MOOR-SCATTER-MED	Comparison to wave buoy mean wave period	Spectral moments (0,2) wave period (Tm02)	INSITU_MED_NRT_OBSERVATIONS_013_035	Merged Quantile-Quantile and Scatter plots between observations and analysis, for all Med, for 1-year period
Evaluation of Med-waves using independent in-situ observations (at buoy locations)				
SWH-H-CLASS2-MOOR-<STAT>-<MOORING ID>	Comparison to wave buoy significant wave height	Spectral significant wave height (Hm0)	INSITU_MED_NRT_OBSERVATIONS_013_035	RMSD, SI, BIAS, CORR, LR_SLOPE, LR_INTR between observations and analysis, for each wave buoy separately, for 1-year period
MWP-H-CLASS2-MOOR-<STAT>-<MOORING ID>	Comparison to wave buoy mean wave period	Spectral moments (0,2) wave period (Tm02)	INSITU_MED_NRT_OBSERVATIONS_013_035	RMSD, SI, BIAS, CORR, LR_SLOPE, LR_INTR between observations and analysis, for each wave buoy separately, for 1-year period
SWH-H-CLASS2-MOOR-QQ-<MOORING ID> SWH-H-CLASS2-MOOR-SCATTER-<MOORING ID>	Comparison to wave buoy significant wave height	Spectral significant wave height (Hm0)	INSITU_MED_NRT_OBSERVATIONS_013_035	Merged Quantile-Quantile and Scatter plots between observations and analysis, for each wave buoy separately, for 1-year period
MWP-H-CLASS2-MOOR-QQ-<MOORING ID> MWP-H-CLASS2-MOOR-SCATTER-<MOORING ID>	Comparison to wave buoy mean wave period	Spectral moments (0,2) wave period (Tm02)	INSITU_MED_NRT_OBSERVATIONS_013_035	Merged Quantile-Quantile and Scatter plots between observations and analysis, for each wave buoy separately, for 1-year period
Evaluation of Med-waves using quasi-independent satellite observations (full MED)				
SWH-H-CLASS4-ALT-<STAT>-MED	Comparison to altimeter significant	Spectral significant wave height (Hm0)	Merged altimeter wave height database from	RMSD, SI, BIAS, CORR, LR_SLOPE, LR_INTR between observations and first-guess, for all Med, for 1-year

	wave height		CERSAT - IFREMER	period and seasonally
SWH-H-CLASS4-ALT-QQ-MED SWH-H-CLASS4-ALT-SCATTER-MED	Comparison to altimeter significant wave height	Spectral significant wave height (Hm0)	Merged altimeter wave height database from CERSAT - IFREMER	Merged Quantile-Quantile and Scatter plots between observations and first-guess, for all Med, for 1-year period
Evaluation of Med-waves using quasi-independent satellite observations (MED sub-regions)				
SWH-H-CLASS4-ALT-<STAT>-<REGION>	Comparison to altimeter significant wave height	Spectral significant wave height (Hm0)	Merged altimeter wave height database from CERSAT - IFREMER	RMSD, SI, BIAS, CORR, LR_SLOPE, LR_INTR between observations and first-guess, for Med sub-basins, for 1-year period
SWH-H-CLASS4-ALT-QQ-<REGION> SWH-H-CLASS4-ALT-SCATTER-<REGION>	Comparison to altimeter significant wave height	Spectral significant wave height (Hm0)	Merged altimeter wave height database from CERSAT - IFREMER	Merged Quantile-Quantile and Scatter plots between observations and first-guess, for Med sub-basins, for 1-year period

Table 4: List of metrics for Med-waves evaluation using in-situ and satellite observations

IV VALIDATION RESULTS

IV.1 Significant wave height

Comparison with in-situ observations

Table 5 shows results of the comparison between analysis SWH (model data) and in-situ observations (reference data), for the Mediterranean Sea as a whole, for the entire year of 2016 and seasonally. In the table, "Entries" refers to the number of model-buoy collocation pairs, i.e. to the sample size available for the computation of the relevant statistics, $\bar{R}$ is the mean reference value, $\bar{M}$ is the mean model value, STD R and STD M are the standard deviations of the reference and model data respectively. The remaining quantities are the qualification metrics defined in the previous section.

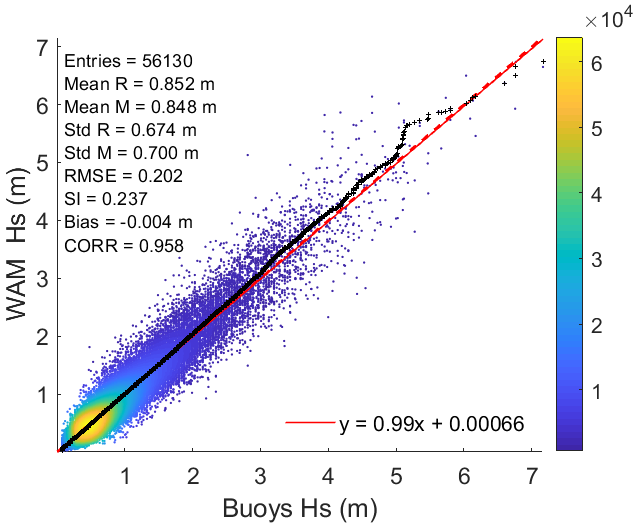

Figure 5 is the respective merged QQ-Scatter plot for the full 1-year period. In the figure, the QQ-plot is depicted with black crosses. Also shown are the best fit line forced through the origin (red solid line) and the 45° reference line (red dashed line).

MED	ENTRIES	$\bar{R}$ (m)	$\bar{M}$ (m)	STD R (m)	STD M (m)	RMSD (m)	SI	BIAS (m)	CORR	LR_SLOPE	LR_INTR
Whole Year	56130	0.852	0.848	0.674	0.700	0.202	0.237	-0.004	0.958	0.995	0.001
Winter	13595	1.050	1.037	0.846	0.889	0.232	0.221	-0.013	0.966	1.015	-0.029
Spring	13349	0.900	0.886	0.617	0.633	0.200	0.221	-0.015	0.950	0.974	0.008
Summer	14297	0.641	0.672	0.469	0.527	0.179	0.275	0.031	0.944	1.060	-0.008
Autumn	14889	0.830	0.812	0.651	0.659	0.194	0.233	-0.018	0.956	0.968	0.009

Table 5: Med-waves SWH evaluation against wave buoys' SWH, for the full Mediterranean Sea, for 1 year period (2016) and seasonally. Relevant metrics from Table 2: SWH-H-CLASS2-MOOR-<STAT>-MED.

Table 5 shows that the typical difference (RMSD) varies from 0.18 m in summer to 0.23 m in winter. However, the scatter in summer (0.27) is about 5% higher than the scatter in winter (0.22) whilst a

lower correlation coefficient is associated with the former season. This suggests that the model follows better the observations in 'stormy' conditions, with well-defined patterns and higher waves. A similar conclusion has been derived by other studies (Cavaleri and Sclavo, 2006; Ardhuin et al., 2007; Bertotti et al., 2013) with respects to wind and wave modelling performance in the Mediterranean Sea. Spring and autumn present similar statistics with spring scatter being better and equal to winter. Small negative bias with a variation of below 1% between seasons is observed for all seasons but summer. In summer, bias is positive and, in terms of relative bias (BIAS/mean(R)), is 7% higher than the largest negative bias observed in autumn. The linear regression slope is also positive in summer with a very small negative intercept indicating a general model overestimation of the observed SWH in this season. A smaller positive slope together with a larger negative intercept and a negative overall bias in winter indicate some model overestimate towards higher waves and model underestimate over the lower wave height range. These results are confirmed by the seasonal QQ-Scatter plots (not shown). Spring and autumn have scatters that are more uniform along the 45° reference line.

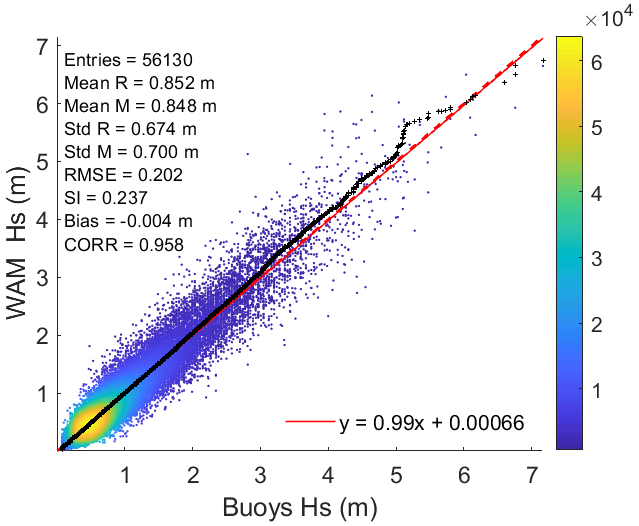

Figure 5: QQ-Scatter plots of Med-waves output SWH (Hs) versus wave buoys' observations, for the full Mediterranean Sea, for 1 year (2016) period: QQ-plot (black crosses), 45° reference line (dashed red line), least-squares best fit line (red line). Relevant metrics from Table 2: SWH-H-CLASS2-MOOR-QQ-MED, SWH-H-CLASS2-MOOR-SCATTER-MED

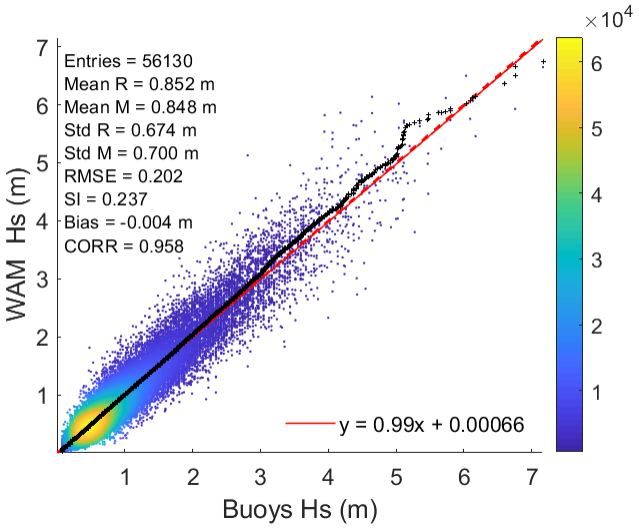

Figure 5 depicts the pattern of the agreement between analysis and observed SWH for different SWH value ranges, for the full Mediterranean Sea. The figure reveals small SWH underestimation by the model mainly for very small wave heights (< 0.6 m). A prevalence of model overestimate is obtained for waves above about 2 m which becomes more pronounced for higher waves.

Table 6 shows results of the comparison between analysis SWH and in-situ observations for each of the wave buoys depicted in **Errore. L'origine riferimento non è stata trovata.**. The

qualification metrics for the different buoy locations (from west to east) are also plotted in

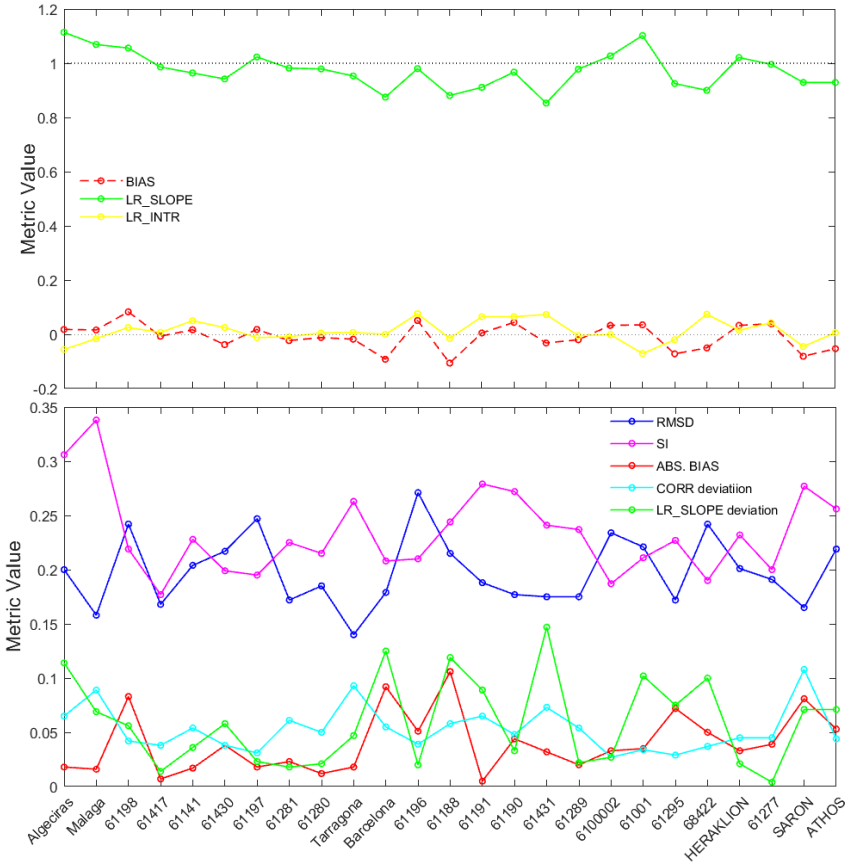

Figure 6 in order to facilitate the visualization and interpretation of the relative performance of the wave model at the different locations. To be able to readily compare the pattern of variation of the different metrics at the different locations the absolute BIAS and the CORR and

LR_SLOPE deviations from unity are plotted in the bottom plot of

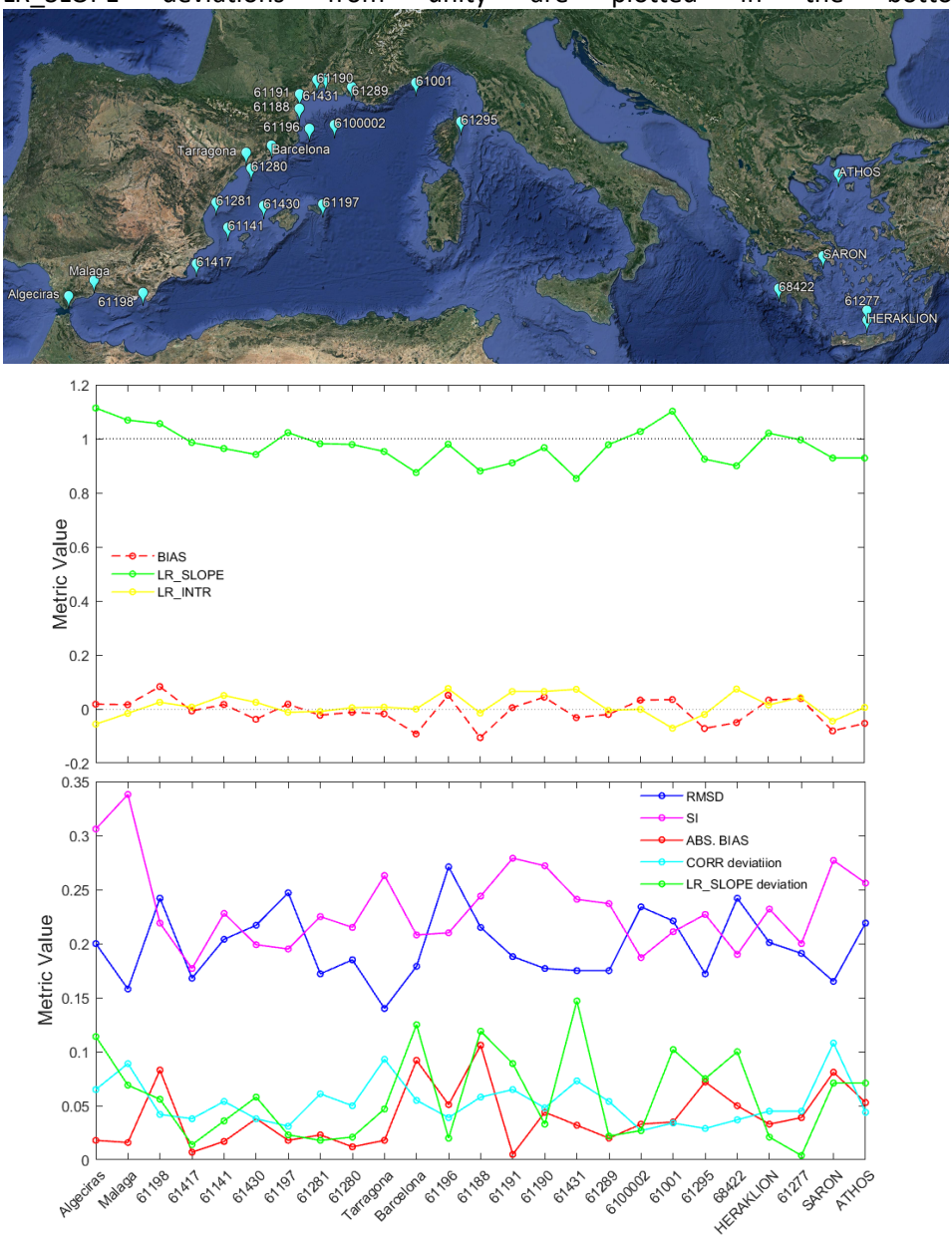

Figure 6. The values of BIAS and LR_SLOPE as given in Table 6 are shown in the middle plot together with LR_INTR. For convenience, a map of the wave buoy locations is included in the figure (top). Finally, Figure 7 shows QQ-Scatter plots at selected locations.

Table 6 and Figure 6 reveal that the typical difference (RMSD) at the different buoy locations varies from 0.14 m to 0.27 m. The Scatter Index (SI) varies from 0.18 at offshore location 61417 (QQ-Scatter in Figure 7) to 0.34 at the coastal buoy of Malaga. In general, SI values above the mean value for the whole Mediterranean Sea (0.24) are obtained at wave buoys located near the coast, particularly if these are sheltered by land masses on their north-northwest (e.g. western French coastline), and/or within enclosed basins characterized by a complex topography such as the Aegean Sea. As explained in several studies (e.g. Cavaleri and Sclavo, 2006; Ardhuin et al., 2007; Bertotti et al., 2013; Zacharioudaki et al., 2015), in these cases, the spatial resolution of the wave model is often not adequate to resolve

the fine bathymetric features whilst the spatial resolution of the forcing wind model is incapable to reproduce the fine orographic effects, introducing errors to the wave analysis. The correlation coefficient (CORR) mostly follows the pattern of variation of the SI. It ranges from 0.89 at SARON (QQ-Scatter in Figure 7) in the Aegean Sea to 0.97 at the deep water buoy 6100002 (QQ-Scatter in Figure 7), offshore from France, which is well exposed to the prevailing north-westerly winds in the region. The BIAS varies from -0.11 m at the coastal buoy 61188 (QQ-Scatter in Figure 7) located near the French-Spanish boarder and backed by the Pyrenees mountains to 0.08 m at offshore location 61198 (QQ-Scatter in Figure 7) in the Alboran Sea. Its sign varies, with positive and negative values computed at almost the same number of locations respectively. Overestimation at buoy 61198 in the Alboran Sea is part of a general overestimation of the wave heights in the Atlantic and Alboran regions as it will be seen later in the comparison with the satellites. The pattern of variation of BIAS generally agrees with the pattern of variation of LR_SLOPE which varies between 0.85 (LR_INTR = 0.07) at the coastal buoy 61431 in the Gulf of Lyon to 1.11 (LR_INTR = -0.06) at the coastal buoy of Algeciras near the Strait of Gibraltar. In most of the cases, when BIAS is negative an LR_SLOPE below unity is obtained pointing to a prevalence of model underestimation of the observed SWH and vice versa. Nevertheless, there are cases when BIAS and LR_SLOPE do not show towards the same direction. In these instances, the LR_INTR is relatively high and points to the same direction as the BIAS. This pattern is indicative of a differential model performance over the different wave height ranges (e.g. buoy 61190, QQ-Scatter in Figure 7) .

Buoy ID	ENTRIES	$\overline{R}$ (m)	$\overline{M}$ (m)	STD R (m)	STD M (m)	RMSD (m)	SI	BIAS (m)	CORR	LR_SLOPE	LR_INTR
Algeciras	2555	0.652	0.67	0.457	0.544	0.2	0.306	0.018	0.935	1.114	-0.056
Malaga	2895	0.465	0.482	0.321	0.377	0.158	0.338	0.016	0.911	1.069	-0.016
61198	2877	1.035	1.118	0.709	0.781	0.242	0.219	0.083	0.958	1.056	0.025
61417	2527	0.951	0.944	0.604	0.618	0.168	0.177	-0.007	0.962	0.986	0.007
61141	2658	0.892	0.91	0.614	0.625	0.204	0.228	0.017	0.946	0.964	0.05
61430	2573	1.076	1.038	0.779	0.763	0.217	0.199	-0.038	0.962	0.942	0.025
61197	2710	1.264	1.282	0.935	0.988	0.247	0.195	0.018	0.969	1.023	-0.012
61281	2520	0.759	0.736	0.471	0.493	0.172	0.225	-0.023	0.939	0.982	-0.009
61280	2796	0.857	0.844	0.572	0.589	0.185	0.215	-0.012	0.95	0.979	0.005
Tarragona	2635	0.528	0.511	0.312	0.327	0.14	0.263	-0.018	0.907	0.953	0.007
Barcelona	2876	0.737	0.645	0.466	0.431	0.179	0.208	-0.092	0.945	0.875	0
61196	2877	1.271	1.321	0.936	0.956	0.271	0.21	0.051	0.961	0.98	0.076
61188	1992	0.768	0.662	0.559	0.523	0.215	0.244	-0.106	0.942	0.881	-0.015
61191	2879	0.673	0.679	0.527	0.514	0.188	0.279	0.005	0.935	0.911	0.065
61190	2904	0.632	0.677	0.552	0.56	0.177	0.272	0.044	0.952	0.967	0.065
61431	1791	0.712	0.681	0.459	0.422	0.175	0.241	-0.032	0.927	0.853	0.073
61289	1465	0.734	0.713	0.518	0.536	0.175	0.237	-0.02	0.946	0.978	-0.005
6100002	1798	1.241	1.273	0.941	0.993	0.234	0.187	0.033	0.973	1.027	-0.001
61001	2812	1.032	1.067	0.701	0.799	0.221	0.211	0.035	0.966	1.102	-0.071
61295	728	0.688	0.616	0.652	0.621	0.172	0.227	-0.072	0.971	0.925	-0.02
68422	834	1.244	1.195	0.872	0.815	0.242	0.19	-0.05	0.963	0.9	0.074
HERAKLION	1211	0.854	0.887	0.627	0.67	0.201	0.232	0.033	0.955	1.021	0.015
61277	1190	0.935	0.974	0.602	0.627	0.191	0.2	0.039	0.955	0.996	0.043
SARON	1380	0.52	0.439	0.302	0.315	0.165	0.277	-0.081	0.892	0.929	-0.045
ATHOS	2647	0.829	0.776	0.725	0.704	0.219	0.256	-0.053	0.956	0.929	0.006

Table 6: Med-waves SWH evaluation against wave buoys' SWH, for each individual buoy location, for 1 year period (2016). Relevant metrics from Table 2: SWH-H-CLASS2-MOOR-<STAT>-<MOORING ID> .

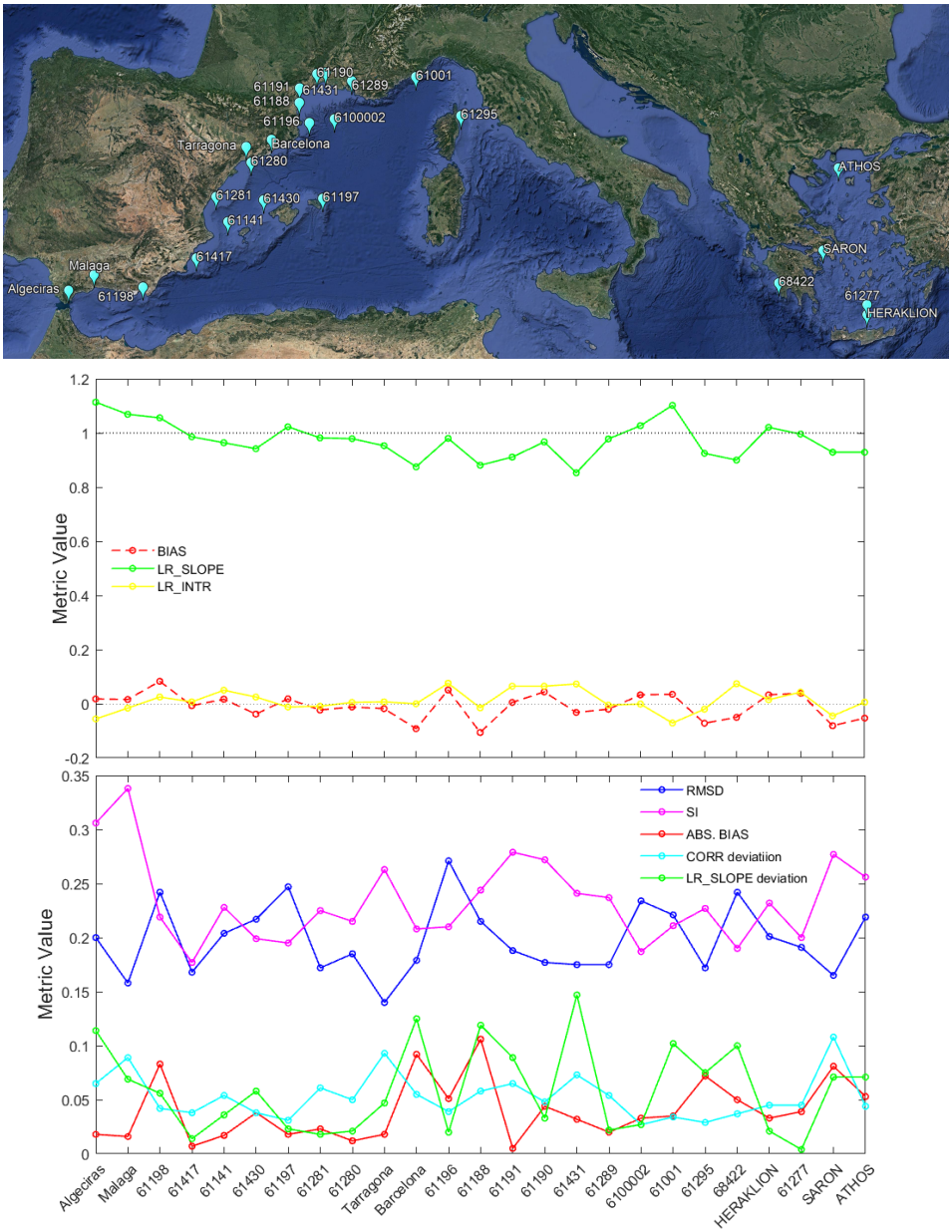

Figure 6: SWH metrics (middle, bottom) at buoy locations (top) for 1 year period (2016) (plots display metrics starting from the western buoy location and moving eastwards. Bottom plot: CORR and LR_SLOPE deviations from unity are shown.

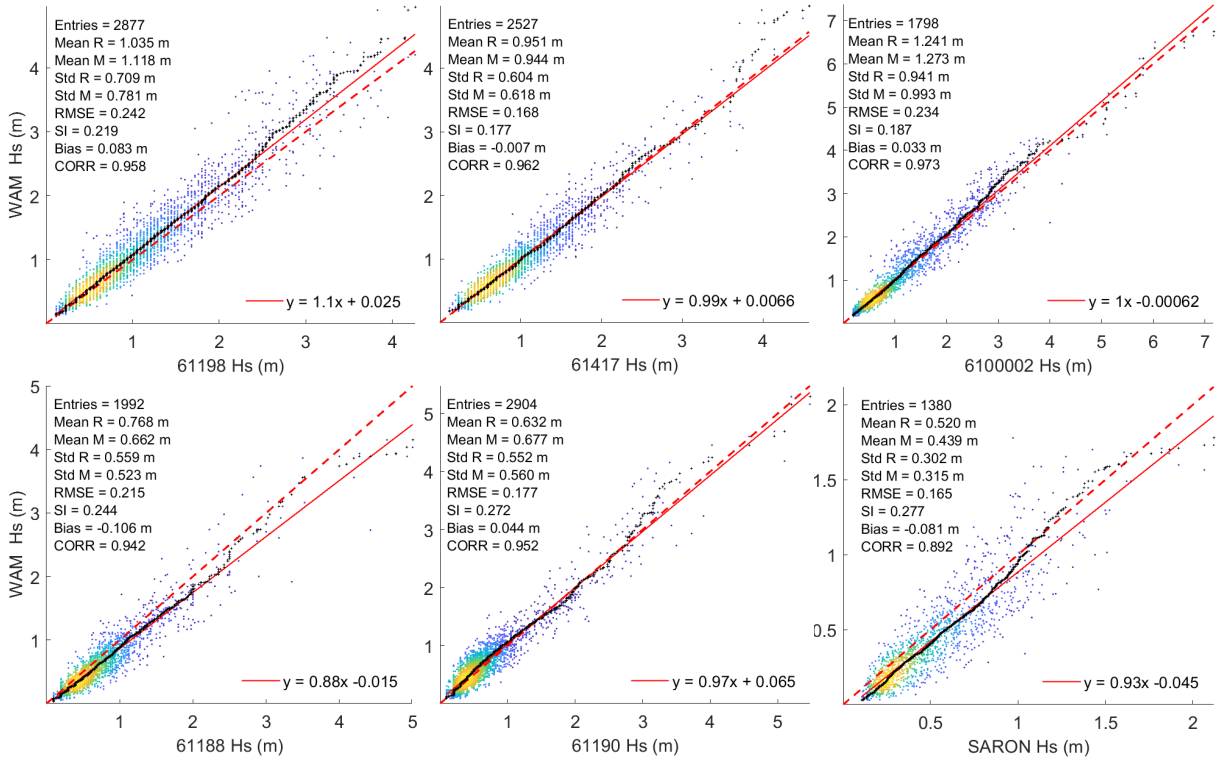

Figure 7: QQ-Scatter plots of Med-waves output SWH (Hs) versus wave buoy observations at specific wave buoy locations, for 1 year (2016) period: QQ-plot (black crosses), 45° reference line (dashed red line), least-squares best fit line (red line). Relevant metrics from Table 2: SWH-H-CLASS2-MOOR-QQ-<MOORING ID>.

Comparison with satellite observations

Table 7 shows statistics from the comparison of the Med-waves first-guess SWH and satellite observations of SWH, for the full Mediterranean Sea, for 1-year period and seasonally. Figure 8 (right) shows the corresponding QQ-Scatter plot for 1-year period, for the full Mediterranean Sea. Figure 8 (left) shows an equivalent QQ-Scatter plot resulting from the comparison of the ECMWF forcing wind speeds, U10, and JASON-2 measurements of U10 (no U10 available from SARAL or CRYOSAT-2).

MED	ENTRIES	$\overline{R}$ (m)	$\overline{M}$ (m)	STD R (m)	STD M (m)	RMSD (m)	SI	BIAS (m)	CORR	LR_SLOPE	LR_INTR
Whole Year	41458	1.180	1.149	0.814	0.823	0.214	0.179	-0.031	0.967	0.977	-0.004
Winter	10665	1.497	1.472	1.024	1.052	0.253	0.168	-0.025	0.971	0.997	-0.021
Spring	10757	1.226	1.197	0.774	0.773	0.217	0.175	-0.029	0.961	0.960	0.020
Summer	10143	0.875	0.857	0.503	0.508	0.171	0.195	-0.018	0.943	0.954	0.023
Autumn	9893	1.101	1.046	0.723	0.717	0.204	0.178	-0.055	0.963	0.956	-0.006

Table 7: Med-waves SWH evaluation against satellite SWH (JASON-2 and SARAL), for the full Mediterranean Sea, for 1 year period (2016) and seasonally. Relevant metrics from Table 2: SWH-H-CLASS4-ALT-<STAT>-MED.

Figure 8 (left) shows that the ECMWF forcing wind model underestimates observed U10 throughout the entire U10 range, even more so at high wind speeds. An overall model underestimation of 9% associated with an LR_SLOPE of 0.82 have been computed. Figure 8 (right) also shows an overall Med-waves model underestimation of observed SWH by about 3% associated with a LR_SLOPE of 0.98. Nevertheless, in this case the model mostly converges to the observed SWH with a slight underestimate over the lower SWH range (< 2,5 m) and some overestimate over higher waves. This apparent discrepancy between wind and wave scatter distributions is a consequence of the modification of the default values of the whitecapping dissipation coefficients in WAM (see Section II.2). A QQ-Scatter obtained before this modification (not shown) is indeed very similar to the one of the ECMWF wind speeds in Figure 8. On the whole, Figure 8 shows that the performance of Med-waves at offshore locations in the Mediterranean Sea (satellite records near the coast are mostly filtered out as unreliable) is very good. Comparing to the equivalent results obtained from the model-buoy comparison (**Errore. L'origine riferimento non è stata trovata.**), a smaller scatter (by about 6%) with a larger overall bias (by about 2.5%) is associated with the model-satellite comparison. SI values compare well at the more exposed wave buoys in the Mediterranean Sea.

Table 7 shows the seasonal variation of the Med-waves model performance. The typical difference (RMSD) varies from 0.17 m in summer to 0.25 m in winter. SI is highest in summer (0.2) and lowest in winter (0.17). Correlation coefficient varies accordingly. In general, as explained in the previous sub-section, a lower scatter with a higher correlation is expected the more well-defined the weather conditions are. The values of SI and CORR are similar in spring and autumn lying somewhat closer to winter than to summer. BIAS is negative in all seasons. Its highest relative value (BIAS/mean(R)) of 5% is computed for autumn and its lowest of about 2% for winter and summer. In accordance, LR_SLOPE is always below unity reaching unity in winter.

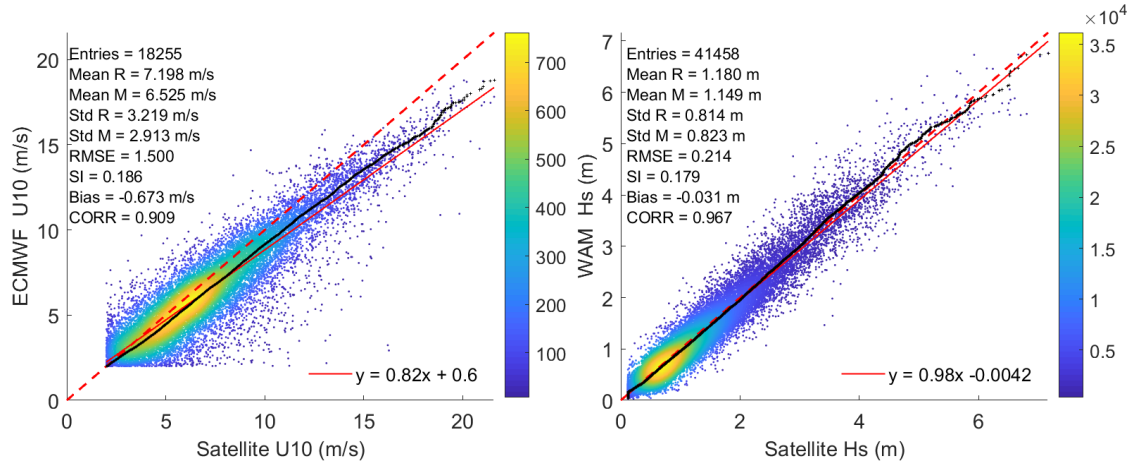

Figure 8: QQ-Scatter plots of: (left) ECMWF forcing wind speed U10 versus satellite U10 (JASON-2); (right) Med-waves SWH (Hs) versus satellite SWH (JASON-2 and SARAL), for the full Mediterranean Sea, for 1 year (2016) period. Relevant metrics from Table 2: SWH-H-CLASS4-ALT-QQ-MED and SWH-H-CLASS4-ALT-SCATTER-MED

Table 8 shows the statistics of the comparison of the Med-waves first-guess SWH and satellite observations of SWH for the different sub-regions of the Mediterranean Sea defined in Figure 1. For visualization purposes, Figure 10 (right column) maps the statistics shown in Table 8. In addition, equivalent statistics are mapped for the ECMWF - satellite comparison of wind speeds (left column). Note that it is the Relative BIAS (BIAS/mean(R)) that is displayed in this figure. This quantity allows for a more straightforward comparison between the different sub-basins in terms of percentage deviations from the observed mean value. It is also highlighted that the spatial coverage of the model-satellite wind collocations (measurements only from JASON-2) is much more limited than the spatial coverage of the model-satellite wave collocations (measurements from both SARAL and JASON-2). As a consequence, the wave statistics are expected to be more representative of the sub-regions under consideration compared to the wind statistics. This is particularly true for the Adriatic, the Ligurian and the Alboran Seas. In addition, the wave statistics have been computed using a sample size of at least 400 data points whilst the wind statistics have been obtained with a minimum sample requirement of 200 data points. Thus, the confidence associated with the wave statistics is higher than the confidence associated with the wind statistics. For the above reasons, the wind metrics presented in Figure 10 are interpreted with caution.

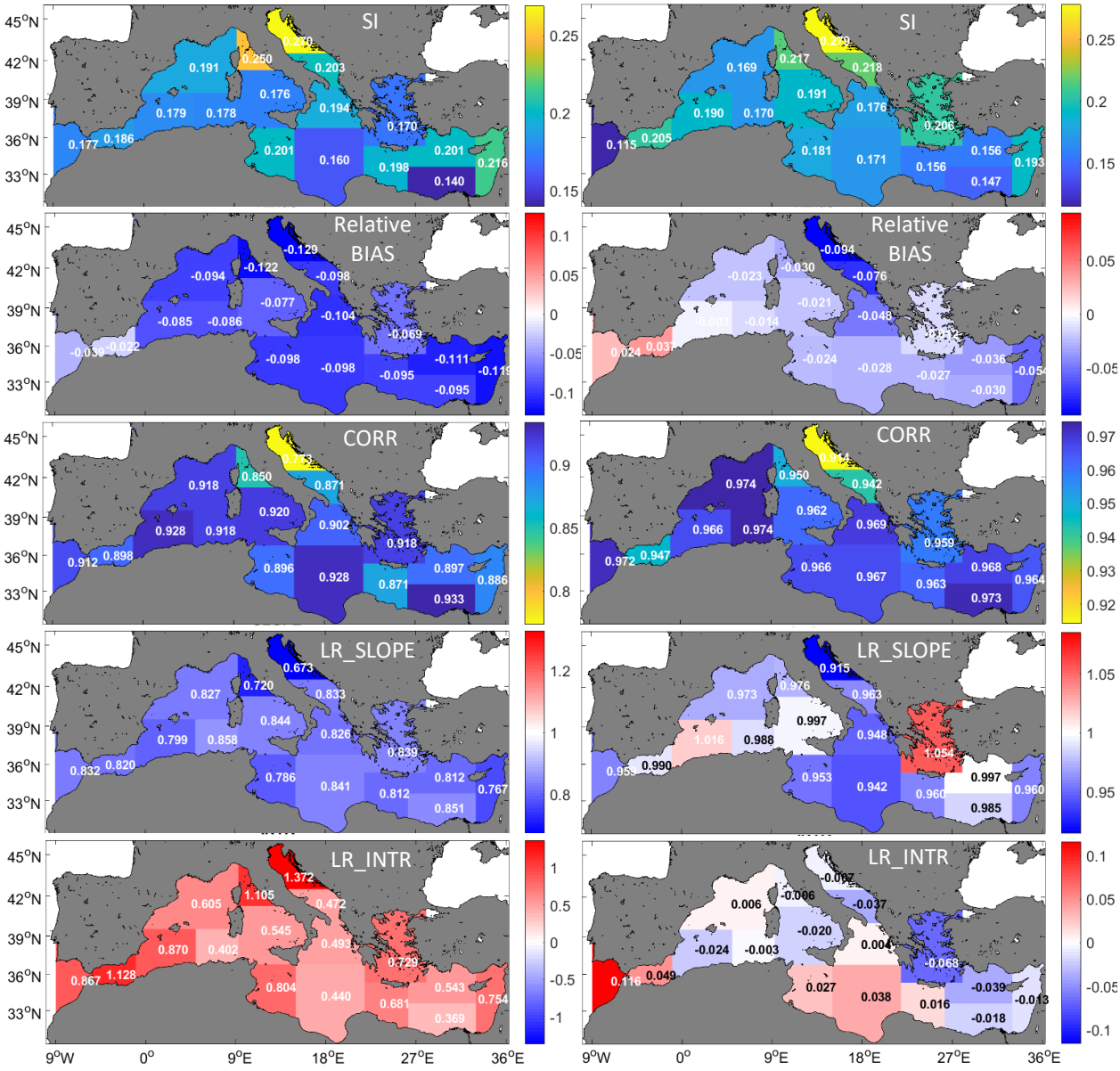

Figure **9** (right column) shows that the highest value of SI is obtained for the North Adriatic Sea (0.28) followed by the South Adriatic and the Ligurian Seas (0.22). The Aegean and Alboran Seas have also relatively high SI values (0.21). The lowest values (0.15-0.16) are found in the west and central Levantine Basin. Relatively low values are also found in the Ionian Sea (0.17-0.18) and west of the islands of Sardinia and Corsica (0.17). SI and CORR have a similar pattern of variation. In accordance with these results, Ratsimandresy et al. (2008), examining model-satellite agreement over coastal locations of the western Mediterranean Sea, found the worst correlations in the Alboran Sea and east of Corsica Island. Bertotti et al. (2013), in a comparison of high resolution wind and wave model output with satellite data over different sub-regions of the Mediterranean Sea, also found the largest scatter and lowest correlations in the Adriatic Sea, followed by the Aegean Sea in his study. In agreement, Zacharioudaki et al. (2015), focusing on the Greek Seas, have shown a considerably larger scatter in the Aegean Sea than in the surrounding seas, when model output was compared to satellite observations.

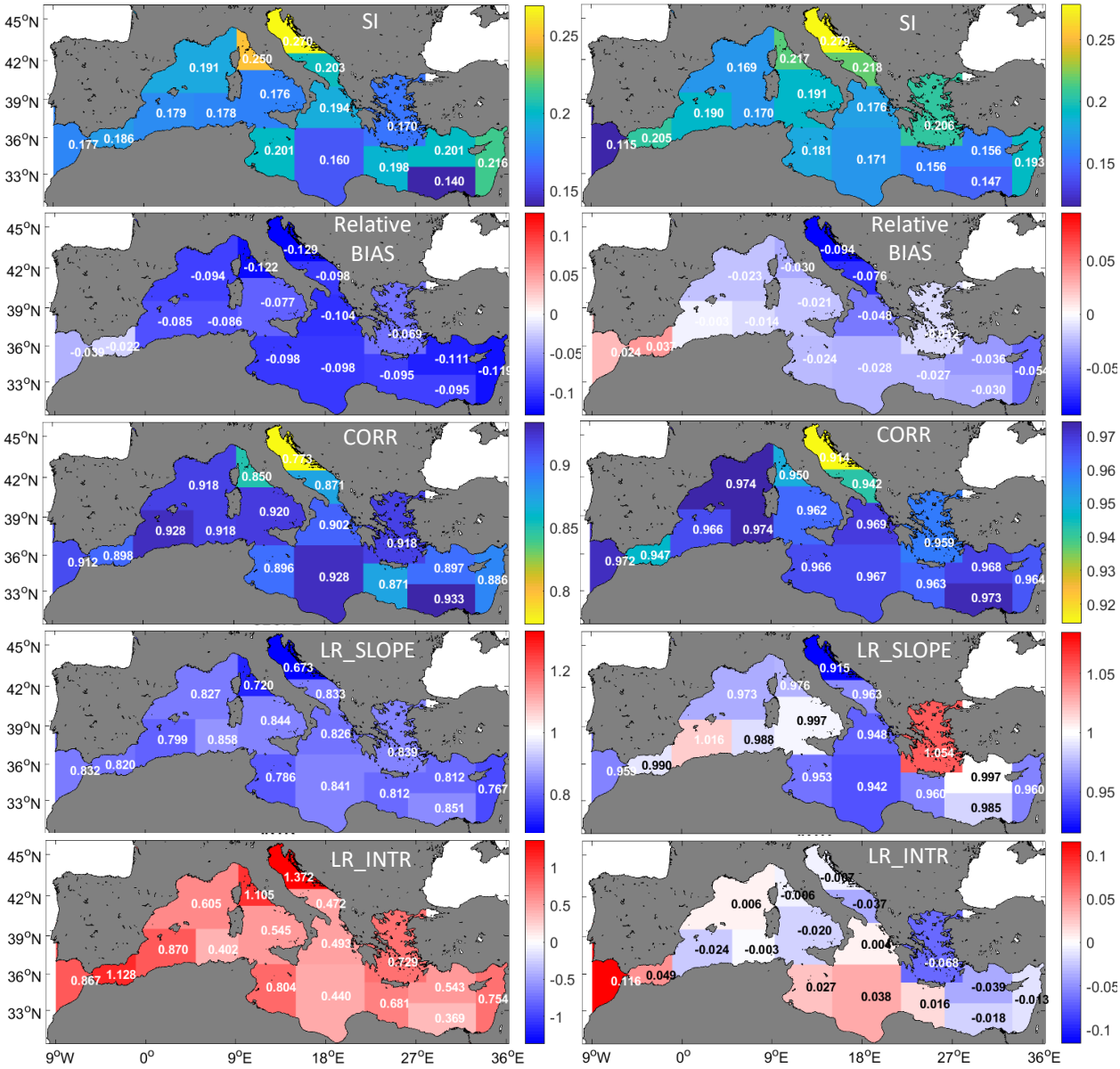

Figure 9: ECMWF U10 (left column) and Med-waves SWH (right column) evaluation against satellite U10 (JASON-2) and satellite SWH (JASON-2 and SARAL) respectively: maps of metric values over the Mediterranean Sea sub-regions shown in Figure 1, for 1 year period (2014).

As explained in the previous sub-section (model-buoy comparison), it is the difficulties of wind models to properly reproduce orographic effects and/or local sea breezes and the difficulties of wave models to appropriately resolve complicated bathymetry that introduce errors in these fetch-limited, enclosed regions, often characterized by a complex topography. Indeed, comparison with the equivalent results for the ECMWF wind speeds confirms these difficulties. For example, the pattern of SI and CORR variation for U10 and SWH have similarities, corroborating the conclusion of many studies that errors in wave height simulations by sophisticated wave models are mainly caused by errors in the generating

Satellite	ENTRIES	$\overline{R}$ (m)	$\overline{M}$ (m)	STD R (m)	STD M (m)	RMSD (m)	SI	BIAS (m)	CORR	LR_SLOPE	LR_INTR
atl	1742	1.790	1.832	0.868	0.857	0.209	0.115	0.043	0.972	0.959	0.116
alb	951	1.062	1.101	0.649	0.679	0.221	0.205	0.039	0.947	0.990	0.049
swm1	2789	1.224	1.220	0.850	0.894	0.232	0.190	-0.004	0.966	1.016	-0.024
swm2	1812	1.421	1.401	1.054	1.068	0.242	0.170	-0.020	0.974	0.988	-0.003
nwm	4754	1.349	1.319	0.991	0.990	0.230	0.169	-0.030	0.974	0.973	0.006
tyr1	768	0.979	0.950	0.657	0.675	0.214	0.217	-0.029	0.950	0.976	-0.006
tyr2	3902	1.118	1.094	0.753	0.780	0.214	0.191	-0.024	0.962	0.997	-0.020
ion1	2732	1.140	1.113	0.799	0.788	0.208	0.181	-0.027	0.966	0.953	0.027
Ion2	6573	1.266	1.230	0.844	0.822	0.219	0.171	-0.035	0.967	0.942	0.038
ion3	2503	1.143	1.088	0.813	0.795	0.208	0.176	-0.055	0.969	0.948	0.004
adr1	921	0.820	0.743	0.552	0.552	0.241	0.279	-0.077	0.914	0.915	-0.007
adr2	1065	0.950	0.877	0.601	0.614	0.219	0.218	-0.072	0.942	0.963	-0.037
lev1	2176	1.255	1.220	0.716	0.714	0.198	0.156	-0.034	0.963	0.960	0.016
lev2	3045	1.168	1.126	0.706	0.727	0.187	0.156	-0.042	0.968	0.997	-0.039
lev3	2622	1.191	1.155	0.744	0.753	0.179	0.147	-0.036	0.973	0.985	-0.018
lev4	2069	0.985	0.932	0.715	0.712	0.198	0.193	-0.053	0.964	0.960	-0.013
aeg	2831	1.040	1.028	0.678	0.745	0.214	0.206	-0.012	0.959	1.054	-0.068

Table 8: Med-waves SWH evaluation against satellite SWH (JASON-2 and SARAL), for each individual Mediterranean Sea sub-region shown in Figure 1, for 1 year period (2016). Relevant metrics from Table 2: SWH-H-CLASS4-ALT-<STAT>-<REGION>.

wind fields (e.g. Komen et al., 1994; Ardhuin et al., 2007). Nevertheless, differences do exist. For instance, the SWH SI in the Aegean Sea is relatively higher than the corresponding U10 SI. This is most probably because in this region of highly complicated bathymetry with many little islands the error of the wave model increases in relation to the error of the wind model. Negative BIAS is the case in all sub-regions except for the Atlantic and Alboran Sea. In the latter regions, the wave model overestimates the observations by 2-4%. The QQ-Scatter plots (not shown) associated with these sub-regions show an extended model overestimate over the lower and middle SWH ranges with a variable pattern of over and underestimation over the higher SWH range. This is indicated by the positive bias, strongly positive intercept and below unity slope obtained for these regions. The lowest overall model underestimate (0-1%) is computed for the South-West Mediterranean (swm1, swm2) and the Aegean Sea. In particular, for the west South-West Mediterranean (swm1) and the Aegean Sea a positive slope is computed together with a significantly negative intercept which, as seen in the respective QQ-Scatter plots, are due to a model underestimate of observed SWH over the lower SWH range and a model overestimate over the higher range. This pattern is also seen in the central Levantine and in the Tyrrhenian Sea where a non trivial negative intercept is accompanied by a slope of almost unity. The overall model underestimate in these regions is 2-4%. Negative overall biases of above 4% are computed for the North Ionian, the Adriatic, and the East Levantine Seas reaching up to 9% in the North Adriatic. In these regions and especially in the Adriatic Sea a more severe model underestimate of the observed SWH extending over almost its entire range is observed in the QQ-Scatter plots and indicated by the low linear regression slope. A prevalence of model underestimation is also seen in the rest of the Ionian Sea and in the west Levantine. Comparing with the equivalent results for the ECMWF wind speed, it is evident that although there are similarities in the Relative BIAS distributions, there are

also considerable differences. In general, in terms of absolute value, the Relative BIAS associated with the wind field is larger than that associated with the wave field except for the Alboran Sea. In fact, in the latter region and in the Atlantic, a change of sign from negative to positive is observed between wind and waves. As already mentioned, this is a consequence of the modification of the whitecapping dissipation coefficients from default values in WAM, which has led to an important offset of the negative BIAS associated with the ECMWF wind speeds, especially over the high SWH range. Thus, in regions where the ECMWF underestimate has been small, as in the Atlantic and the Alboran Sea, modification of the dissipation coefficients has eventually led to an overshoot of the observed SWH. This is a robust pattern obtained for the whole Atlantic area simulated by the nested Med-waves model (up to -18.125° W, Figure 3). These discrepancies are also seen in the LR_SLOPES of the two variables.

IV.2 Mean Wave Period

Comparison with in-situ observations

MED	ENTRIES	$\overline{R}$ (m)	$\overline{M}$ (m)	STD R (m)	STD M (m)	RMSD (m)	SI	BIAS (m)	CORR	LR_SLOPE	LR_INTR
Whole Year	45608	3.963	3.474	0.909	1.039	0.693	0.124	-0.488	0.881	1.007	-0.516
Winter	11455	4.210	3.725	1.026	1.188	0.714	0.124	-0.485	0.898	1.040	-0.655
Spring	11389	4.069	3.573	0.887	1.026	0.696	0.120	-0.496	0.880	1.018	-0.569
Summer	11099	3.651	3.157	0.717	0.837	0.681	0.128	-0.494	0.829	0.967	-0.374
Autumn	11665	3.912	3.433	0.878	0.984	0.680	0.123	-0.479	0.872	0.977	-0.388

Table 9: Med-waves MWP evaluation against wave buoys' SWH, for the full Mediterranean Sea, for 1 year period (2016) and seasonally. Relevant metrics from Table 2: MWP-H-CLASS2-MOOR-<STAT>-MED.

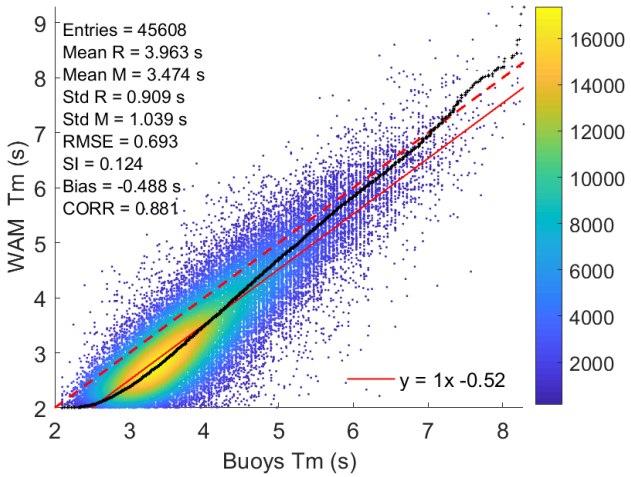

Figure 10: QQ-Scatter plots of Med-waves output MWP (Tm) versus wave buoys' observations, for the full Mediterranean Sea, for 1 year (2016) period. Relevant metrics from Table 2: MWP-H-CLASS2-MOOR-QQ-MED and MWP-H-CLASS2-MOOR-SCATTER-MED

Table 9 presents the statistics of the comparison between the Med-waves analysis mean wave period, MWP, and in-situ observations of mean wave period, for the full Mediterranean Sea, for 1 year period (2016) and seasonally. Figure 10 shows the corresponding QQ-Scatter plot for the year-long statistics. It is shown that the model exhibits greater variability than the observations (STD in Table 9). The RMSD varies from 0.68 s in summer and autumn to 0.71 s in winter. In relation to the mean of the observations (RMSD/mean(R)), the model-observation difference is about 17-19%, with winter, spring and autumn being at the low end of this range and summer at the high. SI variation is minimal and is 0.12-0.13. The non-trivial deviation of SI from relative RMSD (RMSD/mean(R)) indicates that a substantial part of the model-observation difference is caused by BIAS. CORR has its minimum value (0.83) in summer and its maximum (0.9) in winter. As before, these results indicate that the model wave period, like the model wave height, better follows the observations in well-defined wave conditions of higher waves and larger periods. The BIAS is negative with values that correspond to a

model underestimate of about 11-14%. LR_SLOPEs vary from 0.97 in summer to 1.04 in winter with a persistently negative intercept ranging from -0.37 in summer to -0.65 in winter. In agreement, the seasonal QQ-Scatter plots (not shown) show a general tendency of the model to underestimate wave periods except over the higher percentiles where model overestimate (mostly in winter and spring) or some convergence occurs. The year-long QQ-Scatter plot in Figure 10 shows that the wave model underestimates the observations for MWP < 7 s whilst model overestimate is observed for higher periods. Measurements of MWP < 4.5 s are especially underestimated by the model.

Buoy ID	ENTRIES	$\overline{R}$ (m)	$\overline{M}$ (m)	STD R (m)	STD M (m)	RMSD (m)	SI	BIAS (m)	CORR	LR_SLOPE	LR_INTR
Algeciras	2048	3.728	3.249	0.903	1.038	0.764	0.16	-0.479	0.821	0.943	-0.267
Malaga	2646	3.697	3.396	0.734	0.993	0.71	0.174	-0.301	0.762	1.031	-0.416
61198	2896	4.195	3.698	0.822	0.944	0.673	0.108	-0.497	0.877	1.007	-0.527
61417	2523	4.2	3.722	0.747	0.898	0.641	0.102	-0.477	0.88	1.058	-0.723
61430	2582	4.401	3.939	0.934	1.135	0.658	0.106	-0.462	0.915	1.112	-0.956
61197	2711	4.723	4.247	1.085	1.306	0.678	0.102	-0.476	0.935	1.125	-1.069
61281	2505	3.888	3.386	0.721	0.885	0.664	0.112	-0.502	0.873	1.071	-0.777
61280	2811	4.057	3.471	0.751	0.884	0.72	0.103	-0.587	0.882	1.039	-0.744
Tarragona	2581	3.878	3.412	0.855	0.983	0.753	0.152	-0.466	0.802	0.921	-0.161
Barcelona	2502	4.1	3.606	0.84	1.025	0.726	0.13	-0.493	0.855	1.043	-0.671
61196	2868	4.42	3.869	0.884	0.992	0.687	0.093	-0.552	0.911	1.022	-0.649
61188	1928	3.857	3.402	0.849	1.017	0.7	0.138	-0.456	0.853	1.022	-0.539
61191	2491	3.407	2.957	0.865	0.918	0.649	0.137	-0.45	0.864	0.917	-0.166
61190	2528	3.417	2.979	0.902	0.926	0.636	0.135	-0.437	0.872	0.895	-0.08
61431	1616	3.629	2.994	0.694	0.789	0.759	0.114	-0.636	0.851	0.968	-0.52
61289	1343	3.636	3.104	0.669	0.743	0.705	0.128	-0.532	0.789	0.877	-0.085
61295	658	3.75	3.295	0.859	1.007	0.659	0.127	-0.455	0.881	1.033	-0.58
68422	830	4.53	4.122	0.974	1.11	0.594	0.096	-0.407	0.922	1.051	-0.64
HERAKLION	1183	3.685	3.516	0.79	0.989	0.498	0.127	-0.168	0.885	1.107	-0.561
61277	1178	3.916	3.49	0.671	0.799	0.603	0.109	-0.426	0.845	1.006	-0.451
SARON	920	3.158	2.586	0.384	0.5	0.671	0.112	-0.571	0.711	0.925	-0.336
ATHOS	2260	3.938	3.171	0.784	0.845	0.845	0.09	-0.767	0.908	0.978	-0.68

Table 10: Med-waves MWP evaluation against wave buoys' MWP, for each individual buoy location, for 1 year period (2016). Relevant metrics from Table 2: MWP-H-CLASS2-MOOR-<STAT>-<MOORING ID>.

Table 10 gives the statistics of the model-buoy comparison at individual wave buoy locations (Figure 11, top). Figure 11, alike Figure 6, plots those statistics to facilitate their visualization and interpretation. Figure 12 shows QQ-Scatter plots at selected locations.

The typical model-observation difference (RMSD) varies from 0.5 s to 0.85 s. Relative to the mean of the observations (RMSD/mean(R)), this variation corresponds to a percentage range of 13% (68422, HERAKLION) - 21% (ATHOS, SARON). SI is relatively small with values between 0.1 (ATHOS, 68422) and 0.17 (Malaga) while CORR varies from 0.71 (SARON) to 0.94 (61197). Generally, similarly to the wave height results, the lowest correlations are found at coastal locations affected by fetch differences between model and reality due to a complex surrounding topography. On the other hand, the highest correlations are obtained at the most exposed locations in Figure 11 (top). For example, location 68422 which is very well-exposed to the prevailing westerly fetches scores very well in all of the aforementioned metrics. In Figure 11, it is evident that the RMSD is mainly caused by BIAS which is

negative at all locations and varies between about 5 % (HERAKLION) and 20% (ATHOS). In agreement with BIAS, LR_INTR is negative everywhere. Its range is -1.07 (61197) to -0.08 (61190). Nevertheless, LR_SLOPE is often above unity which, as seen in the QQ-Scatter plots, is due to the tendency of model MWP to convergence or even overestimate the observed MWP over the higher MWP range. LR_SLOPE variation is 0.88 (61289) to 1.13 (61197).

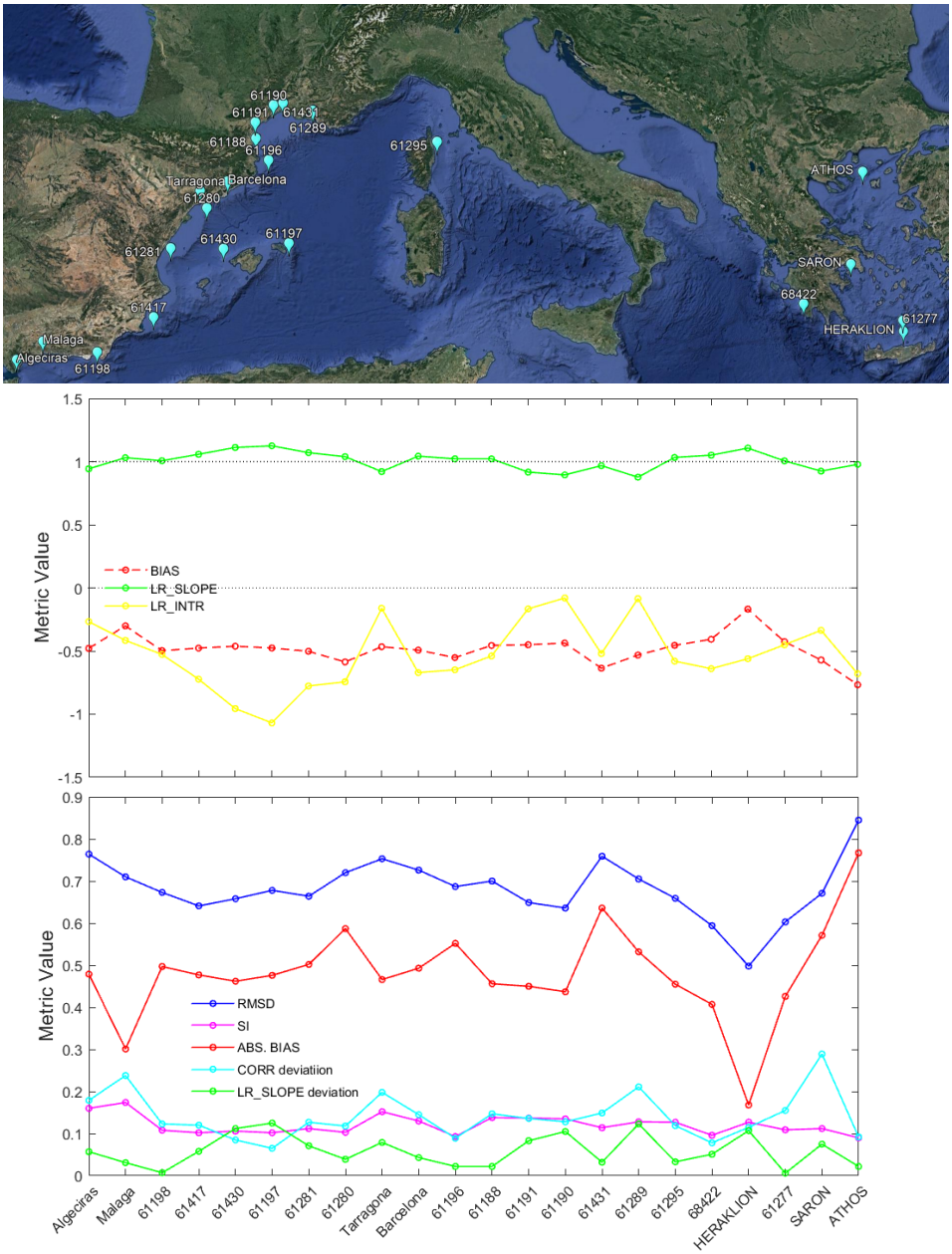

Figure 11: MWP metrics (bottom) at buoy locations (top) for 1 year period (2016) (plots display metrics starting from the western buoy location and moving eastwards. Last value corresponds to the full Mediterranean Sea). CORR and LR_SLOPE deviations from unity are shown.

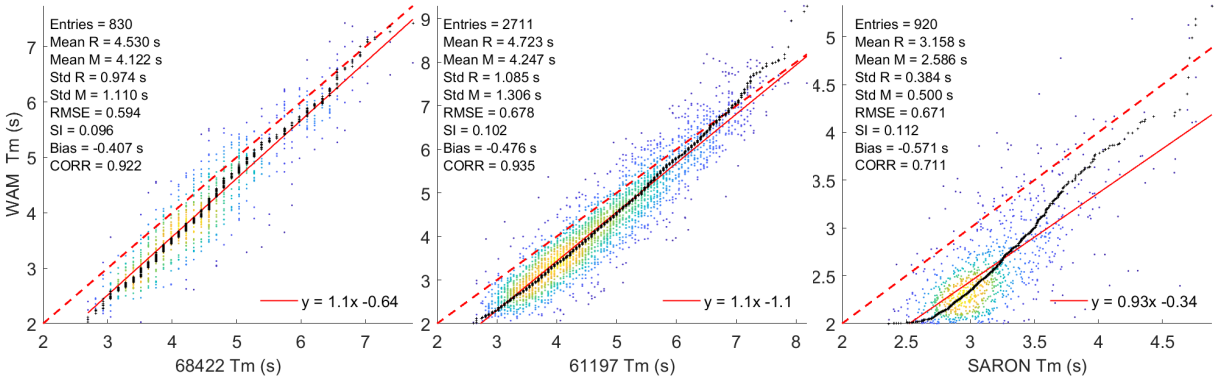

Figure 12: QQ-Scatter plots of Med-waves output MWP (Tm) versus wave buoy observations at specific wave buoy locations, for 1 year (2016) period: QQ-plot (black crosses), 45° reference line (dashed red line), least-squares best fit line (red line). Relevant metrics from Table 2: SWH-H-CLASS2-MOOR-QQ-<MOORING ID>.

V SYSTEM'S NOTICEABLE EVENTS, OUTAGES OR CHANGES

V.1 Q2/2018 to Q1/2019

The changes of the previous version (Q1/2019) of the CMEMS Med-waves system compared to its preceding one (Q2/2018) are:

- Upgrade to WAM Cycle 4.6.2 with inclusion of non-linear wave-wave interactions for shallow water.
- Tuning of the wave age parameter (zalp = 0.011 from default value 0.008).
- Imposition of a limitation to the high frequency part of the spectrum based on Phillips spectrum:

$$F_{PH}(f) = a_{PH} g^2 (2\pi)^{-4} f^{-5}$$

where,

a_{PH} : dimensionless equilibrium range coefficient for Phillips spectral (a_{PH} is set to 0.03)

g : gravitational acceleration

f : cyclic frequency

This change has been already implemented in the wave component of ECMWF IFS CY43R1 (ECMWF, 2016) and it is expected to reduce the wave steepness in high wind conditions.

- Inclusion of CRYOSAT-2 and SARAL/Altika along-track SWH observations to the data assimilation scheme.

V.2 Q1/2019 to Q1/2020

The new version of the Med-waves system (Q1/2020) differs from the previous one (Q1/2019) as regards the time of the daily forecast cycle, starting in the new version at 00:00 UTC (instead of 12:00 UTC). This technical change does not affect the quality of the product. Also, the new version assimilates data from one more satellite (SENTINEL-3B). Relevant quality changes are described in the following section.

VI QUALITY CHANGES SINCE PREVIOUS VERSION

The impact of the additional assimilation of SENTINEL-3B SWH observations on Med-waves SWH quality was evaluated by performing two sensitivity runs over a 6-month period (14/03/2019 – 20/09/2019): one assimilated SWH observations from four satellites (Q1/2019) excluding SENTINEL-3B and the other additionally assimilated SENTINEL-3B data. Analysis and first-guess output was compared to in-situ and satellite observations respectively. In the second case, the comparison was done against the four satellites already assimilated in the previous version of the system.

The results showed marginal differences in quality introduced by the additional assimilation of SENTINEL-3B SWH. In particular, in the Mediterranean Sea and its sub-regions, an improvement of up to 0.5% was computed whilst locally, at wave buoy locations, differences of less than ± 0.5% were mostly detected reaching up to 1% at very few locations. Locally, quality improvement was more often observed than deterioration.

VII REFERENCES

Alves, J.H.G.M., 2006. Numerical modeling of ocean swell contributions to the global wind-wave climate. Ocean Model. 11, 98–122.

Ardhuin, F., Bertotti, L., Bidlot, J.R., Cavaleri, L., Filipetto, V., Lefevre, J.M., Wittmann, P., 2007. Comparison of wind and wave measurements and models in the Western Mediterranean Sea. Ocean Eng. 34, 526–541.

Bertotti, L., Cavaleri, L., Loffredo, L., Torrisi, L., 2013. Nettuno: Analysis of a Wind and Wave Forecast System for the Mediterranean Sea. Mon. Weather Rev. 141, 3130–3141.

Cavaleri, L., Sclavo, M., 2006. The calibration of wind and wave model data in the Mediterranean Sea. Coast. Eng. 53, 613–627.

ECMWF, 2016. ifs.documentation CY43R1. Part VII: ECMWF Wave - Model documentation 2016. URL https://www.ecmwf.int/en/elibrary/17120-part-vii-ecmwf-wave-model

Galil, B., Herut, B., Rosen, D.S., Rosentroup, Z., 2006. A Consise Physical, Chemical and Biological Characterizasion of Eastern Mediterranean with Emphasis on the Israeli coast. IOLR Report H07.

Gerling, W.T., 1992. Partitioning Sequences and Arrays of the Directional Ocean Wave Spectra into Component Wave Systems. J. Atmos. Oceanic Tech. 9, 444-458.

Günther, H., Behrens, A., 2012. The WAM model. Validation document Version 4.5.4. Intitute of Coastal Research Helmholtz-Zentrum Geesthach (HZG).

Hasselmann, K., 1974. On the spectral dissipation of ocean waves due to white capping. Boundary-Layer Meteorol. 6, 107–127.

Hasselmann, K., Barnett, T.P., Bouws, E., Carlson, H., Cartwright, D.E., Enke, K., Ewing, J.A., Gienapp, H., Hasselmann, D., Kruseman, P., Meerburg, A., Müller, P., Olbers, D.J., Richter, K., Sell, W., Walden, H., 1973. Measurements of wind-wave growth and swell decay during the Joint North Sea Wave Project (JONSWAP). Deutches Hydrographisches Institut. 8.

Hasselmann, S., Hasselmann, K., 1985. Computations and Parameterizations of the Nonlinear Energy Transfer in a Gravity-Wave Spectrum. Part I: A New Method for Efficient Computations of the Exact Nonlinear Transfer Integral. J. Phys. Oceanogr. 15, 1369–1977.

Hasselmann, S., Hasselmann, K., Allender, J., Barnett, T., 1985. Computations and Parameterizations of the Nonlinear Energy Transfer in a Gravity-Wave Specturm. Part II: Parameterizations of the Nonlinear Energy Transfer for Application in Wave Models. J. Phys. Oceanogr. 15, 1378–1391.

Janssen, P., 1989. Wave-Induced Stress and the Drag of Air Flow over Sea Waves. J. Phys. Oceanogr. 19, 745–754.

Janssen, P., 1991. Quasi-linear Theory of Wind-Wave Generation Applied to Wave Forecasting. J. Phys. Oceanogr. 21, 1631–1642.

Komen, G.J., Cavaleri, L., Donelan, M., Hasselmann, K., Hasselmann, S., Janssen, P., 1994. Dynamics and modelling of ocean waves. Cambridge University Press.

Queffeulou, P., Croizé-Fillon, D., 2013. Glogal altimeter SWH data set - May 2013. Technical Report. URL ftp://ftp.ifremer.fr/ifremer/cersat/products/swath/altimeters/waves/documentation/.

Queffeulou, P., OSTST 2016, Validation of Jason-3 altimeter wave height measurements.

Ratsimandresey, A.W., Sotillo,M.G., Carretero Albiach, J.C., Álvarez Fanjul, E., Hajji, H., 2008. A 44-year high-resolution ocean and atmospheric hindcast for the Mediterranean Basin developed within the HIPOCAS Project. Coast. Eng. 55, 827–842.

Ravdas, M., Zacharioudaki, A. and Korres, G.: Implementation and validation of a new operational wave forecasting system of the Mediterranean Monitoring and Forecasting Centre in the framework of the Copernicus Marine Environment Monitoring Service, Nat. Hazards Earth Syst. Sci., 18(10), 2675–2695, doi:10.5194/nhess-18-2675-2018, 2018.

Semedo, A., Sušelj, K., Rutgersson, A., Sterl, A., 2011. A Global View on the Wind Sea and Swell Climate and Variability from ERA-40. J. Clim. 24, 1461–1479.

Sepulveda, H.H., Queffeulou, P., Ardhuin, F., 2015. Assessment of SARAL/AltiKa Wave Height Measurements Relative to Buoy, JASON-2, and Cryosat-2 Data. Mar. Geod. 38, 449–465.

Snyder, R.L., Dobson, F.W., Elliott, J.A., Long, R.B., 1981. Array measurements of atmospheric pressure fluctuations above surface gravity waves. J. Fluid Mech. 102, 1-59.

WAMDI Group, 1988. The WAM Model—A Third Generation Ocean Wave Prediction Model. J. Phys. Oceanogr. 18, 1775–1810.

Young, I.R., 1999. Seasonal variability of the global ocean wind and wave climate. Int. J. Climatol. 19, 931–950.

Zacharioudaki, A., Korres, G., Perivoliotis, L., 2015. Wave climate of the Hellenic Seas obtained from a wave hindcast for the period 1960 – 2001. Ocean Dyn. 65, 795–816.